Critical and tricritical points for the massless 2D Gross-Neveu model beyond large N

Jean-Loïc Kneur,[1,*] Marcus Benghi Pinto,[2,†] and Rudnei O. Ramos[3,‡]

[1]*Laboratoire de Physique Mathématique et Théorique–CNRS–UMR 5825 Université Montpellier II, France*
[2]*Departamento de Física, Universidade Federal de Santa Catarina, 88040-900 Florianópolis, Santa Catarina, Brazil*
[3]*Departamento de Física Teórica, Universidade do Estado do Rio de Janeiro, 20550-013 Rio de Janeiro, RJ, Brazil*

(Received 17 October 2006; published 27 December 2006)

Using optimized perturbation theory, we evaluate the effective potential for the massless two-dimensional Gross-Neveu model at finite temperature and density containing corrections beyond the leading large-N contribution. For large N, our results exactly reproduce the well-known $1/N$ leading order results for the critical temperature, chemical potential, and tricritical points. For finite N, our critical values are smaller than the ones predicted by the large-N approximation and seem to observe Landau's theorem for phase transitions in one space dimension. New analytical results are presented for the tricritical points that include $1/N$ corrections. The easiness with which the calculations and renormalization are carried out allied to the seemingly convergent optimized results displayed, in this particular application, show the robustness of this method and allows us to obtain neat analytical expressions for the critical as well as tricritical values beyond the results currently known.

DOI: 10.1103/PhysRevD.74.125020 PACS numbers: 11.10.Wx, 11.15.Tk, 12.38.Cy

I. INTRODUCTION

The study of symmetry breaking/restoration in quantum field theories is an important issue of relevance in many areas of physics. For example, today, problems regarding phase transitions in Bose-Einstein condensates (BEC) or in quantum chromodynamics (QCD) concentrate a lot of theoretical as well as experimental efforts.

Of topical importance regarding studies of phase transitions in quantum field theory is the reliability of perturbation theory and its eventual breakdown. For instance, perturbation theory at high temperatures breaks down due to the appearance of large infrared divergences, happening, for example, in massless field theories, like in QCD [1], close to critical temperatures (in field theories displaying a second order phase transition or a weakly first order transition [2,3]), or just because at high temperatures there are parameter regimes where conventional perturbation schemes become unreliable when powers of the coupling constants become surmounted by powers of the temperature. In these cases, a nontrivial problem arises since nonperturbative methods must be used. Various nonperturbative techniques have been used to deal with these problems. Among them, we will be particularly interested in the $1/N$ approximation [4] which, here, will be considered mainly for comparison. Though a powerful resummation method, the $1/N$ approximation can quickly become cumbersome after the resummation of the first leading contributions, like, for example, in $N = 2$ (e.g., BEC and polyacetylene) or $N = 3$ (e.g., QCD) finite N problems. This is due to technical difficulties such as the formal resummation of infinite subsets of Feynman graphs and their subsequent renormalization.

An alternative nonperturbative analytical method that we will make use of in this work is the optimized perturbation theory, or linear δ expansion (LDE) [5]. In calculational terms (including renormalization) its appeal regards the fact that one remains within the framework of perturbation theory. Then, nonperturbative results are obtained by optimizing the perturbatively evaluated quantities. This procedure amounts to eliminating, variationally, mass parameters used to deform (interpolate) the original action. Recently, the LDE has been successful in treating scalar field theories at finite temperature and/or density. Relativistic scalar $\lambda\phi^4$ theories have been treated at finite temperature [6] as well as at finite temperature and density [7]. At the same time, their nonrelativistic counterpart, which is relevant for BEC, has been studied in connection with the problem of the dependence with interactions of the critical temperature shift ΔT_c, given by the difference between the interacting and ideal gas critical temperatures (for a recent review see, for instance, [8] and references therein). It suffices to say that the latest LDE results [9] are in excellent agreement with the Monte Carlo results, considered the most accurate prediction for ΔT_c, and they perform much better than the $1/N$ expansion used at leading and at next-to-leading order, or NLO (for a review on the different results and methods used to study the ΔT_c in the BEC problem, see [10]). Moreover, the convergence properties for this critical theory have been proved by us and by other authors [9,11,12].

The present work will focus on the LDE applications to problems involving phase transitions in asymptotically free models at finite temperatures and densities. Here, we shall consider the $1 + 1$ dimensional Gross-Neveu model (GN), which is extensively used as a prototype model in studies related to phase transitions in particle physics as well as condensed matter physics. One recent application concerning particle physics is the next-to-leading order

*Electronic address: kneur@lpta.univ-montp2.fr
†Electronic address: marcus@fsc.ufsc.br
‡Electronic address: rudnei@uerj.br

in $1/N$ evaluation of the effective potential at finite temperature performed in Ref. [13]. In the condensed matter domain, a very interesting recent application of the GN model was to the study of polymers [14], where a *massive* version of the model was used to show the appearance of a kink-antikink crystal phase that was missed in a previous work [15].

In Ref. [14] the authors work only within the leading order of the $1/N$ expansion, so their results still show a phase transition at finite temperature T and density μ. On the other hand, they consider the case of inhomogeneous background fields, which should be physically more relevant in the $1+1$ dimensional GN model. This is so because, in one space dimension, due to the Landau-Mermin-Wagner-Coleman theorem [16–18], no phase transition related to a discrete symmetry breaking (in this case a discrete chiral symmetry in the massless GN model considered in this work) is expected at any finite temperature. In the GN model, this can be explained by the role played by kinklike inhomogeneous configurations [19] that come to dominate the action functional, instead of just homogeneous, constant field configurations. By accounting for kinklike configurations in the large-N approximation, the authors of Ref. [14] (see also Ref. [20] for a review) find evidence for a crystal phase that shows up in the extreme $T \sim 0$ and large μ part of the phase diagram. The other extreme of the phase diagram, large T and $\mu \sim 0$, remains identical to the usual large-N results for the critical temperature and tricritical points, which are well-known results [21–23]. In the study performed here, we only consider homogeneous backgrounds, but go beyond large N, so the phase diagram changes as a whole. However, we cannot see any crystal phase at small μ that should be a consequence of kinklike configurations dominating the action functional at that extreme of the phase diagram. Despite this, we are still improving the calculations for the GN model even though we are not considering inhomogeneous fields. And, as explained above, since inhomogeneous backgrounds do not seem to change appreciably the large T and small μ region, up to the tricritical point of the phase diagram, we are certainly improving the knowledge in that part of the phase diagram. At the same time, we believe that our results are not faithful in the small T and large μ part of the phase diagram, which gets affected at large by inhomogeneous backgrounds as shown by the results obtained for the GN model in the large-N approximation [14], though no results beyond large N are currently available. Eventually, in the future it would be opportune to contrast the results found by the authors of Ref. [14], who considered a inhomogeneous background field to evaluate the effective action, with the ones provided by the LDE in the same context so that it could generate the effects of kink configurations beyond the large N limit considered in Ref. [14].

Another purpose of the work done here is to show the advantages and reliability of an alternative nonperturbative method like the LDE in the understanding of the phase diagram of the massless GN model when considered beyond the large-N limit. In this case, the massless GN model provides an excellent testing framework for the following reasons. As mentioned in the previous paragraph, large-N results for the critical temperature (T_c) [21], critical chemical potential (μ_c) [22], and tricritical points [15] are well known [23]. At the same time, Landau's theorem [16,19] for phase transitions states that they cannot occur in one space dimension, so that rigorously $T_c = 0$, meaning that the large-N approximation behaves poorly in this case. These two extreme results allow us to gauge the LDE performance in connection with the problem, since we know that for $N \to \infty$ our results should converge to the ''exact'' large-N result. For finite N, on the other hand, our results should predict smaller values for the critical temperatures, in accordance with Landau's theorem. At zero temperature and density, the LDE has been applied to this model with some success [24,25], since in this simpler case the LDE could even be summed to all perturbative orders (at least in the $1/N$ approximation), so that the large order behavior of the LDE could be investigated. In fact, its convergence properties have been proved for a particular perturbation series in this context [25]. At finite temperature, an early application to the GN model [26] showed the potentiality of this method. However, the renormalization program has not been addressed in Ref. [26]. Here, our aim is to use all the latest LDE improvements to evaluate the GN effective potential at finite temperature and density for any value of N.

This work is organized as follows. In Sec. II we present the LDE method and the interpolated GN model. For illustrative purposes we evaluate the effective potential for $N \to \infty$. We show, in accordance with Ref. [27], that, when correctly applied, the LDE exactly reproduces, already at first order, the large-N results. The situation is unchanged, at any order in δ, provided that one stays within the $N \to \infty$ limit. This nice result is valid for any parameter values. In the same section, we explicitly evaluate the $1/N$ correction that also appears at the first LDE nontrivial order. In Sec. III the LDE order-δ results are presented and compared to the large-N results for the four situations described above. Our major result is the production of analytical relations for the fermionic mass, critical temperature, and critical chemical potential, as well as tricritical points containing a finite N correction. We show that all these quantities depend on an optimized mass scale set by the LDE. All the analytical expressions have been cross checked numerically. In Sec. IV we contrast the LDE and the $1/N$ approximation results to leading order and to next-to-leading order. Our conclusions are presented in Sec. V. Two appendixes are included to show some technical details and the renormalization for the interpolated model.

II. THE GROSS-NEVEU MODEL AND THE EFFECTIVE POTENTIAL FOR THE INTERPOLATED THEORY

The Gross-Neveu model is described by the Lagrangian density for a fermion field ψ_k ($k = 1, \ldots, N$) given by [28]

$$\mathcal{L} = \bar{\psi}_k(i\partial\!\!\!/)\psi_k + m_F\bar{\psi}_k\psi_k + \frac{g^2}{2}(\bar{\psi}_k\psi_k)^2, \tag{2.1}$$

where the summation over flavors is implicit in the above equation, with e.g. $\bar{\psi}_k\psi_k = \sum_{k=1}^{N}\bar{\psi}_k\psi_k$. Since we restrict ourselves to the two-dimensional space-time dimension, ψ_k represents a two-component Dirac spinor for each value of the flavor index k. When $m_F = 0$ the theory is invariant under the discrete transformation

$$\psi \rightarrow \gamma_5\psi, \tag{2.2}$$

displaying a discrete chiral symmetry (CS). In addition, Eq. (2.1) has a global $SU(N)$ flavor symmetry.

For the studies of the model, Eq. (2.1), in the large-N limit, it is convenient to define the four-fermion interaction as $g^2N = \lambda$. Since g^2 vanishes like $1/N$, we study the theory in the large-N limit with fixed λ (see e.g. [29]).

Let us now turn our attention to the implementation of the LDE procedure within the GN model. According to the usual LDE interpolation prescription [5] (for a long, but far from complete list of references on the method, see [30]), from the *original* four-fermion theory, Eq. (2.1), we define the deformed theory,

$$\mathcal{L}_\delta(\psi, \bar{\psi}) = \bar{\psi}_k(i\partial\!\!\!/)\psi_k + \eta(1-\delta)\bar{\psi}_k\psi_k + \delta\frac{\lambda}{2N}(\bar{\psi}_k\psi_k)^2, \tag{2.3}$$

so that at $\delta = 0$ we have a theory of free fermions. Now, the introduction of an auxiliary scalar field σ can be achieved by adding the quadratic term

$$-\frac{\delta N}{2\lambda}\left(\sigma + \frac{\lambda}{N}\bar{\psi}_k\psi_k\right)^2 \tag{2.4}$$

to $\mathcal{L}_\delta(\psi, \bar{\psi})$. We are then led to the interpolated model

$$\mathcal{L}_\delta = \bar{\psi}_k(i\partial\!\!\!/)\psi_k - \delta\sigma\bar{\psi}_k\psi_k - \eta(1-\delta)\bar{\psi}_k\psi_k - \frac{\delta N}{2\lambda}\sigma^2. \tag{2.5}$$

Details of the renormalization process for the interpolated model are given in Appendix B. Note that the same interpolation of the form (2.5) was also used in Ref. [31], but it is different from the ones used in Refs. [26,27,32]. In those references the interpolation was not carried out in the original four-fermion theory but on its bosonized version. However, we argue that the present choice is more adequate because at $\delta = 0$ one has only free fermions. (This is equivalent to the interpolation defined when considering only fermionic fields, as performed e.g. in Refs. [24,33], which also consistently defines a free theory for $\delta \rightarrow 0$.) However, with the alternative approach, the quadratic bosonic term $\sigma^2/(2\lambda)$ survives at $\delta = 0$ and the theory looks to be composed by free fermions and bosons which is misleading since, by the equations of motion, $\sigma = (\lambda/N)\bar{\psi}_k\psi_k$. There are also some quantitative differences in the results obtained from using our present interpolation and the alternative ones performed in Refs. [26,27,32]. For instance, within the latter, one only reproduces the $N \rightarrow \infty$ result at the first LDE order, and the first nontrivial finite N corrections only appear at order δ^2. At the same time, our approach appears to converge faster by producing finite $1/N$ corrections already at the first LDE order since the σ propagator is proportional to $1/\delta$. From the Lagrangian density in the interpolated form, Eq. (2.5), we can immediately read the corresponding new Feynman rules in Minkowski space. Each Yukawa vertex carries a factor $-i\delta$, while the (free) σ propagator is now $-i\lambda/(N\delta)$. The LDE dressed fermion propagator is

$$S_F(p) = \frac{i}{p\!\!\!/ - \eta_* + i\epsilon}, \tag{2.6}$$

where $\eta_* = \eta - (\eta - \sigma_c)\delta$ with σ_c representing a constant scalar field background around which σ in Eq. (2.5) is expanded.

Any quantity computed from the above rules, at some finite order in δ, is dependent on the parameter η, which then must be fixed somehow. Here, as in most of the previous references on the LDE method, η is fixed by using the principle of minimal sensitivity (PMS). In the PMS procedure one requires that a physical quantity $\Phi^{(k)}$, that is calculated perturbatively to some kth order in δ, be evaluated at the point where it is less sensitive to this parameter. This criterion then translates into the variational relation [34]

$$\left.\frac{d\Phi^{(k)}}{d\eta}\right|_{\bar{\eta},\delta=1} = 0. \tag{2.7}$$

The optimum value $\bar{\eta}$ that satisfies Eq. (2.7) must be a function of the original parameters, including the couplings, thus generating nonperturbative results.

The effective potential to order δ: going beyond the large-N limit

Let us now show how the optimization procedure implemented by the LDE improves over the large-N results. Here we revert to the usual LDE procedure by expanding the effective potential in powers of δ only. This quantity can be expressed in terms of the full fermionic self-energy, whose terms contributing up to order δ^2 are displayed in Fig. 1. The second diagram in Fig. 1 represents a correction to the σ propagator, while the third has corrections to the Yukawa vertex. The first and fourth are exchange (rainbow) types of graphs.

The corresponding contributions to the effective potential up to order δ^2 are shown in Fig. 2. This nicely illus-

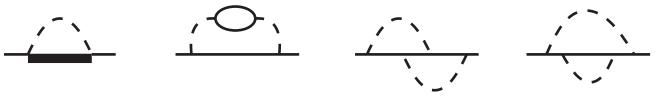

FIG. 1. Contributions to the fermion self-energy up to order δ^2. The continuous thick line represents the LDE, η_* dependent, dressed fermion propagator, while the thin lines represent the η dependent propagators. The dashed line represents the scalar auxiliary field, σ. Tadpole diagrams are not shown since they do not contribute to V_{eff}.

trates how the LDE incorporates, at the same perturbative order, graphs that have different N dependence.

The leading order term, represented by the first diagram in Fig. 2, is also the only one that survives in the large-N limit. Then, upon using the Feynman rules from the interpolated model (2.5), one finds

$$\frac{V_{\text{eff}}}{N}(\sigma_c, \eta_*, N \to \infty) = \delta\frac{\sigma_c^2}{2\lambda} + i\int\frac{d^dp}{(2\pi)^d}\,\text{tr}\ln(\not{p} - \eta_*). \tag{2.8}$$

Already in the large-N limit, Eq. (2.8) contains *arbitrary* orders in δ [26,27,31] through $\eta_* = \eta - (\eta - \sigma_c)\delta$. All standard large-$N$ results [29] can be obtained by simply setting $\delta = 1$ and performing the replacement $\eta_* \to \sigma_c$ in (2.8).

It is instructive to develop Eq. (2.8) to first order in δ to show some subtle points associated with the LDE method and, in particular, to see how the optimization procedure defined by Eq. (2.7) works. Expanding Eq. (2.8) to first order in δ, one obtains

$$\frac{V_{\text{eff},\delta^1}}{N}(\sigma_c, \eta, N \to \infty) = \delta\frac{\sigma_c^2}{2\lambda} + i\int\frac{d^dp}{(2\pi)^d}\,\text{tr}\ln(\not{p} - \eta) + \delta i\int\frac{d^dp}{(2\pi)^d}\,\text{tr}\frac{\eta - \sigma_c}{\not{p} - \eta + i\epsilon}. \tag{2.9}$$

Fixing $\delta = 1$, we now optimize V_{eff} for η, which is done by applying Eq. (2.7) directly to the effective potential. Applying the PMS to Eq. (2.9) immediately gives the result $\bar{\eta} = \sigma_c$, which then recovers *exactly* the large-N result. This same trend holds at any temperature and/or density, any value of the coupling λ, and any number of space-time

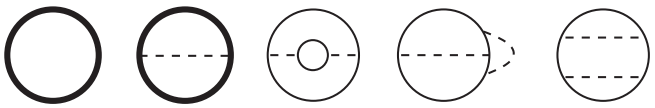

FIG. 2. Feynman diagrams contributing to the effective potential up to order δ^2. Note that the second and third diagrams have a $1/N$ dependence while the last two have a $1/N^2$ dependence. The thick lines in the first two graphs represent the LDE, η_*, propagators which, as discussed in the text, must be further expanded to order δ^2.

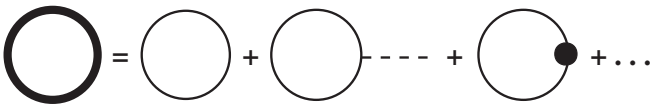

FIG. 3. Diagrammatic relation between Eqs. (2.8) and (2.9). The thick continuous line on the left-hand side represents the LDE dressed fermionic propagator which is η_* dependent. The first diagram on the right-hand side is an order-δ^0 vacuum graph. The dashed line represents the auxiliary field, σ_c, while the black dot stands for the $\delta\eta$ vertex. The last two graphs on the right-hand side are of order δ.

dimensions since there is no need to perform the integrals explicitly. Also, as shown in Ref. [27], the inclusion of higher order terms does not spoil this nice result, provided we stay within the large-N limit, since they are all of the form $\delta^k f_k(\eta - \sigma_c)^k$, where $k \geq 2$. Note that the PMS admits another solution given by

$$\frac{d}{d\eta}\left[\int\frac{d^dp}{(2\pi)^d}\,\text{tr}\frac{i}{\not{p} - \eta + i\epsilon}\right]_{\bar{\eta}} = 0. \tag{2.10}$$

However, this solution, which depends only on scales introduced by the regularization process, and thus is not proportional to the basic scale of the model after dimensional transmutation ($Me^{-\pi/\lambda}$), can be taken as unphysical [27] since it brings no information about the theory being studied.

One can spot a subtle point associated with the LDE evaluation of the effective potential by looking at the diagrams considered to order δ in Eq. (2.9). These graphs are displayed in Fig. 3, which shows the diagrammatic relation between Eqs. (2.8) and (2.9). Note that Eq. (2.9) contains two σ_c independent (vacuum) terms that would be neglected in most evaluations since they are irrelevant as far as CS breaking/restoration is concerned. However, as pointed out in Ref. [27], they are η dependent and so must be considered until the theory is optimized. One can also easily see that, in fact, those contributions are responsible for the quick LDE convergence towards the exact large-N result already at the first nontrivial order.

Let us now consider the second diagram of Fig. 2. This contribution, which is to be summed with Eq. (2.8), reads

$$\frac{V^{(a)}_{\text{eff},\delta^1}}{N}(\eta_*) = -i\frac{1}{2}\int\frac{d^2p}{(2\pi)^2}\,\text{tr}\left[\frac{\Sigma_a(\eta_*)}{\not{p} - \eta_* + i\epsilon}\right], \tag{2.11}$$

where the trace is over Dirac matrices only.[1] The term Σ_a represents the first contribution of Fig. 1 to the fermion self-energy,

$$\Sigma_a(\eta_*) = -\delta\left(\frac{\lambda}{N}\right)i\int\frac{d^2q}{(2\pi)^2}\frac{1}{\not{q} - \eta_* + i\epsilon}. \tag{2.12}$$

[1]The factor -1 corresponding to a closed fermionic loop has already been taken into account [35].

Originally, Root [35] summed up all $1/N$ corrections to next-to-leading order, and, by further perturbatively expanding his result, one easily retrieves Eq. (2.11).

Then, from the equations given in Appendix A at finite temperature and density and by performing the resulting momentum space integrals in (2.11), one finds, after taking the trace and renormalizing with the fermionic mass counterterm (see also Appendix B), the finite result for Eq. (2.11) is

$$\frac{V^{(a)}_{\mathrm{eff},\delta^1}}{N}(\sigma_c, \eta_*, T, \mu) = \delta\frac{\lambda}{4\pi^2 N}\left\{\eta_*^2\left[\ln\left(\frac{M}{\eta_*}\right) - I_2(\eta_*/T, \mu/T)\right]^2 + T^2 J_2^2(\eta_*/T, \mu/T)\right\}, \quad (2.13)$$

where

$$I_2(a, b) = -2\frac{\partial I_1(a, b)}{\partial a^2} = \int_0^\infty \frac{dx}{\sqrt{x^2+a^2}}\left(\frac{1}{e^{\sqrt{x^2+a^2}+b}+1} + \frac{1}{e^{\sqrt{x^2+a^2}-b}+1}\right). \quad (2.14)$$

The function $I_1(a, b)$ is defined as

$$I_1(a, b) = \int_0^\infty dx[\ln(1+e^{-\sqrt{x^2+a^2}-b}) + \ln(1+e^{-\sqrt{x^2+a^2}+b})], \quad (2.15)$$

while the function $J_2(a, b)$ in Eq. (2.13) is defined by

$$J_2(a, b) = \sinh(b)\int_0^\infty dx \frac{1}{\cosh(\sqrt{x^2+a^2})+\cosh(b)}. \quad (2.16)$$

The (finite) contributions given by the term proportional to $I_2(a, b)$ and $J_2(a, b)$ originate from the summation over Matsubara frequencies of the T and μ dependent contributions, more precisely, from Eqs. (A2) and (A3), respectively (see Appendix A for details). Note that the divergence is only contained, at this order, in the $T = 0$, $\mu = 0$ part, which is renormalized by standard counterterms in the $\overline{\mathrm{MS}}$ scheme (see Appendix B for details).

Finally, by summing the contribution, Eq. (2.13), to the effective potential expression to leading order in N, Eq. (2.9), and expanding the resulting expression, one obtains the complete LDE expression to order δ,

$$\frac{V_{\mathrm{eff},\delta^1}}{N}(\sigma_c, \eta, T, \mu) = \delta\frac{\sigma_c^2}{2\lambda} - \frac{1}{2\pi}\left\{\eta^2\left[\frac{1}{2}+\ln\left(\frac{M}{\eta}\right)\right] + 2T^2 I_1(\eta/T, \mu/T)\right\} + \delta\frac{\eta(\eta-\sigma_c)}{\pi}\left[\ln\left(\frac{M}{\eta}\right) - I_2(\eta/T, \mu/T)\right] + \delta\frac{\lambda}{4\pi^2 N}\left\{\eta^2\left[\ln\left(\frac{M}{\eta}\right) - I_2(\eta/T, \mu/T)\right]^2 + T^2 J_2^2(\eta/T, \mu/T)\right\}. \quad (2.17)$$

Notice once more, from Eq. (2.17), that our first order takes into account the first next-to-leading order correction to the large-N result.

When considering the case $T = 0$, $\mu \neq 0$ in Eq. (2.17), one can take the limit $T \to 0$, which then gives for the functions I_1, I_2, and J_2 the results

$$\lim_{T\to 0} T^2 I_1(\eta/T, \mu/T) = -\frac{1}{2}\theta(\mu-\eta)\left[\eta^2\ln\left(\frac{\mu+\sqrt{\mu^2-\eta^2}}{\eta}\right) - \mu\sqrt{\mu^2-\eta^2}\right], \quad (2.18)$$

$$\lim_{T\to 0} I_2(\eta/T, \mu/T) = \theta(\mu-\eta)\ln\left(\frac{\mu+\sqrt{\mu^2-\eta^2}}{\eta}\right), \quad (2.19)$$

$$\lim_{T\to 0} T J_2(\eta/T, \mu/T) = \mathrm{sgn}(\mu)\theta(\mu-\eta)\sqrt{\mu^2-\eta^2}. \quad (2.20)$$

Note that all the above results vanish for $\mu < \eta$. When considering the case $T \neq 0$ and $\mu = 0$ the high-temperature limit, $\eta/T \ll 1$ and $\mu/T \ll 1$, will prove to be useful. For I_1, this approximation follows from the result of expanding Eq. (2.15) in powers of a and b. This result is finite and given by [36]

$$I_1(a \ll 1, b \ll 1) = \frac{\pi^2}{6} + \frac{b^2}{2} - \frac{a^2}{2}\ln\left(\frac{\pi}{a}\right) - \frac{a^2}{4}(1-2\gamma_E) - \frac{7\zeta(3)}{8\pi^2}a^2\left(b^2+\frac{a^2}{4}\right) + \mathcal{O}(a^2b^4, a^4b^2), \quad (2.21)$$

where $\zeta(3) \simeq 1.202$. For I_2, analogously, it can be obtained using Eq. (2.14), which yields

$$I_2(a \ll 1, b \ll 1) = \ln\left(\frac{\pi}{a}\right) - \gamma_E + \frac{7\xi(3)}{4\pi^2}\left(b^2 + \frac{a^2}{2}\right) + \mathcal{O}(a^4, b^4). \tag{2.22}$$

In the general case of $T \neq 0$ and $\mu \neq 0$, the integrals I_1, I_2, and J_2 will be handled numerically.

III. OPTIMIZATION AND NUMERICAL RESULTS BEYOND LARGE N

Before proceeding to the specific $d = 2$ case, considered in this work, let us apply the PMS to the most general order-δ effective potential which is given by

$$\frac{V_{\text{eff},\delta^1}}{N}(\sigma_c, \eta) = \delta\frac{\sigma_c^2}{2\lambda} + i\int\frac{d^dp}{(2\pi)^d}\,\text{tr}\ln(\not{p} - \eta) + \delta i\int\frac{d^dp}{(2\pi)^d}\,\text{tr}\frac{\eta - \sigma_c}{\not{p} - \eta + i\epsilon} + \frac{\delta\lambda}{2N}\,\text{tr}\left[i\int\frac{d^dp}{(2\pi)^d}\frac{1}{\not{p} - \eta + i\epsilon}\right]^2. \tag{3.1}$$

This exercise will help the reader to visualize the way the LDE-PMS resums the perturbative series. After taking the traces in Eq. (3.1) one obtains

$$\frac{V_{\text{eff},\delta^1}}{N}(\sigma_c, \eta) = \delta\frac{\sigma_c^2}{2\lambda} + i\int\frac{d^dp}{(2\pi)^d}\ln(p^2 - \eta^2) + 2\delta i\int\frac{d^dp}{(2\pi)^d}\frac{\eta(\eta - \sigma_c)}{p^2 - \eta^2 + i\epsilon} + \delta\frac{\lambda}{N}\eta^2\left[i\int\frac{d^dp}{(2\pi)^d}\frac{1}{p^2 - \eta^2 + i\epsilon}\right]^2 + \delta\frac{\lambda}{N}\left[i\int\frac{d^dp}{(2\pi)^d}\frac{p_0}{p^2 - \eta^2 + i\epsilon}\right]^2. \tag{3.2}$$

Then, setting $\delta = 1$ and applying the PMS, one gets

$$0 = \left\{\left[\eta - \sigma_c + \eta\frac{\lambda}{N}\left(i\int\frac{d^dp}{(2\pi)^d}\frac{1}{(p^2 - \eta^2 + i\epsilon)}\right)\right]\times\left(1 + \eta\frac{d}{d\eta}\right)\left[i\int\frac{d^dp}{(2\pi)^d}\frac{1}{(p^2 - \eta^2 + i\epsilon)}\right] + \frac{\lambda}{N}\left(i\int\frac{d^dp}{(2\pi)^d}\frac{p_0}{(p^2 - \eta^2 + i\epsilon)}\right)\frac{d}{d\eta}\times\left(i\int\frac{d^dp}{(2\pi)^d}\frac{p_0}{(p^2 - \eta^2 + i\epsilon)}\right)\right\}\Bigg|_{\eta=\bar{\eta}}. \tag{3.3}$$

As one can see in Appendix A [Eq. (A3)], the last term of the equation above only survives when $\mu \neq 0$. In the case $\mu = 0$, Eq. (3.3) factorizes in a nice way which allows us to understand the way the LDE-PMS procedure resums the series producing nonperturbative results. With this aim one can easily check that (at $\delta = 1$)

$$\Sigma_a(\mu, \eta, T) = -\frac{\lambda}{N}\eta\left[i\int\frac{d^dp}{(2\pi)^d}\frac{1}{(p^2 - \eta^2 + i\epsilon)}\right]. \tag{3.4}$$

Then, when $\mu = 0$ the PMS equation factorizes to

$$[\bar{\eta} - \sigma_c - \Sigma_a(\mu = 0, \eta, T)]\left(1 + \eta\frac{d}{d\eta}\right)\times\left[i\int\frac{d^dp}{(2\pi)^d}\frac{1}{(p^2 - \eta^2 + i\epsilon)}\right] = 0, \tag{3.5}$$

which leads to the self-consistent relation

$$\bar{\eta} = \sigma_c + \Sigma_a(\mu = 0, \eta, T), \tag{3.6}$$

which is valid for any temperature and any number of space-time dimensions. In this way the LDE fermionic loops get dressed by σ_c as well as rainbow (exchange) types of self-energy terms like the first graph of Fig. 2. Typical optimized Feynman graphs are shown in Fig. 4. The graphs in Fig. 4(a) represent the order-δ contributions prior to optimization, while the infinite set shown in Fig. 4(b) represents the nonperturbative optimized result. Note how the graphs are dressed by rainbow types of self-energy contributions. This was expected since at order δ the perturbative LDE effective potential receives information about this type of topology only. If one proceeds to order δ^2, information about corrections to the scalar propagator as well as the Yukawa vertex (see Fig. 1) will enter the perturbative effective potential. Then the PMS will dress up these perturbative contributions and so on. In other words, the simple evaluation of a first topologically distinct graph will bring nonperturbative information concerning that type of contribution. Figure 4 clearly shows that the LDE-PMS resums all powers of $1/N$ corresponding to the (rainbow) class of the graph.

Note that the mathematical possibility

$$i\int\frac{d^dp}{(2\pi)^d}\frac{1}{(p^2 - \bar{\eta}^2 + i\epsilon)} = 0 \tag{3.7}$$

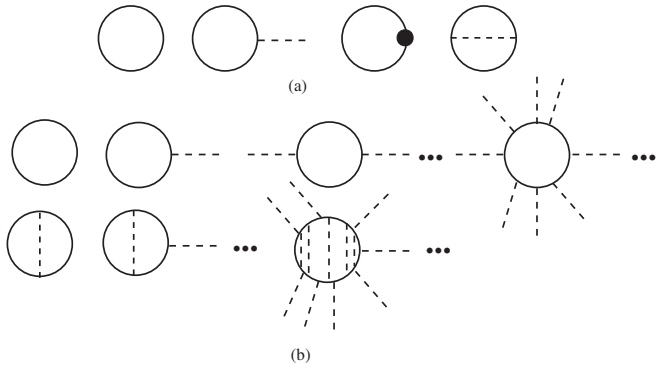

FIG. 4. (a) Feynman diagrams contributing to the effective potential at order δ prior to optimization. (b) The infinite set of graphs contributing to the optimized effective potential.

corresponds to the unphysical solution discussed previously, Eq. (2.10).

Having illustrated the way the LDE-PMS resummation works, let us concentrate on the $d = 2$ case by collecting our results for the complete order-δ effective potential, Eq. (2.17), once the optimization equation is applied to it. Using the PMS procedure, we then obtain, from Eq. (2.17) at $\eta = \bar{\eta}$, the general result

$$\left\{\left[\mathcal{Y}(\eta, T, \mu) + \eta\frac{d}{d\eta}\mathcal{Y}(\eta, T, \mu)\right] \times\left[\eta - \sigma_c + \eta\frac{\lambda}{2\pi N}\mathcal{Y}(\eta, T, \mu)\right] + \frac{\lambda T^2}{2\pi N}J_2(\eta/T, \mu/T)\frac{d}{d\eta}J_2(\eta/T, \mu/T)\right\}\Bigg|_{\eta=\bar{\eta}} = 0, \quad (3.8)$$

where we have defined the function

$$\mathcal{Y}(\eta, T, \mu) = \ln\left(\frac{M}{\eta}\right) - I_2(\eta/T, \mu/T). \quad (3.9)$$

Equation (3.8) expresses our general PMS result, Eq. (3.3), for the specific $d = 2$ case. This can be easily seen by recalling that in this number of space dimensions (and $\delta = 1$) the exchange (Fock) type of self-energy is given by

$$\Sigma_a(\eta, T, \mu) = -\eta\frac{\lambda}{2\pi N}\mathcal{Y}(\eta, T, \mu). \quad (3.10)$$

In the following we will present the analytical (whenever possible) and numerical results for Eq. (3.8). For convenience, the results will be presented in units of M for different values of λ and N. We start by analyzing the simplest case of zero temperature and density.

A. The $T = \mu = 0$ case

Taking Eq. (3.8) at $T = \mu = 0$ [that is, $\mathcal{Y}(\eta, T = 0, \mu = 0) = \ln(M/\eta)$], one gets

$$\left[\ln\left(\frac{M}{\bar{\eta}}\right) - 1\right]\left[\bar{\eta} - \sigma_c - \bar{\eta}\frac{\lambda}{2\pi N}\ln\left(\frac{\bar{\eta}}{M}\right)\right] = 0. \quad (3.11)$$

As discussed previously, the first factor leads to the coupling independent result, $\bar{\eta} = M/e$, which we shall neglect. At the same time, the second factor in (3.11) leads to a self-consistent gap equation for $\bar{\eta}$, given by

$$\bar{\eta}_{\delta^1}(\sigma_c) = \sigma_c\left[1 - \frac{\lambda}{2\pi N}\ln\left(\frac{\bar{\eta}_{\delta^1}}{M}\right)\right]^{-1}. \quad (3.12)$$

The solution for $\bar{\eta}_{\delta^1}$ obtained from Eq. (3.12) is

$$\bar{\eta}_{\delta^1}(\sigma) = -\frac{2\pi N}{\lambda}W^{-1}\left[-\frac{2\pi N}{\lambda}\frac{\sigma_c}{M}\exp\left(-\frac{2\pi N}{\lambda}\right)\right]\sigma, \quad (3.13)$$

where $W(x)$ is the Lambert W (implicit) function [37], which satisfies $W(x)\exp[W(x)] = x$.

To analyze CS breaking, we then replace η by Eq. (3.13) in Eq. (2.17), which is taken at $T = 0$ and $\mu = 0$. As usual, CS breaking appears when the effective potential displays minima at some particular value $\bar{\sigma}_c \neq 0$ which is obtained by minimizing the resulting effective potential with respect to σ_c,

$$\frac{\partial V_{\text{eff},\delta^1}(\sigma_c, \eta = \bar{\eta}_{\delta^1})}{\partial\sigma_c}\Bigg|_{\delta=1,\sigma_c=\bar{\sigma}_c} = \frac{\bar{\sigma}_c}{\lambda} + \frac{1}{\pi}\bar{\eta}\ln\frac{\bar{\eta}}{M} = 0. \quad (3.14)$$

Since $m_F = \bar{\sigma}_c$, after some algebraic manipulation of Eq. (3.14) using the definition of the $W(x)$ function, we find

$$m_{F,\delta^1}(0) = \bar{\sigma}_c(T = 0, \mu = 0) = M\mathcal{F}(\lambda, N)\left(1 - \frac{1}{2N}\right)^{-1}, \quad (3.15)$$

where we have defined the quantity $\mathcal{F}(\lambda, N)$ as

$$\mathcal{F}(\lambda, N) = \exp\left\{-\frac{\pi}{\lambda[1 - 1/(2N)]}\right\}. \quad (3.16)$$

Equation (3.15) is our result for the fermionic mass at first order in δ which goes beyond the large-N result,

$$m_F(0) = \bar{\sigma}_c = M\exp\left(-\frac{\pi}{\lambda}\right). \quad (3.17)$$

Note also that, in the $N \to \infty$ limit, since $\mathcal{F}(\lambda, N \to \infty) = \exp(-\pi/\lambda)$, Eq. (3.15) correctly reproduces, within the LDE nonperturbative resummation, the large-N result. In Fig. 5 we compare the order-δ LDE-PMS results for $\bar{\sigma}_c$ with the one provided by the large-N approximation.

At the same time, $\bar{\eta}$ evaluated at $\bar{\sigma}_c(T = 0, \mu = 0)$, to first order in δ, also follows analytically from Eqs. (3.13) and (3.15),

$$\bar{\eta}_{\delta^1}(\bar{\sigma}_c) = \left(1 - \frac{1}{2N}\right)\bar{\sigma}_c = M\mathcal{F}(\lambda, N). \quad (3.18)$$

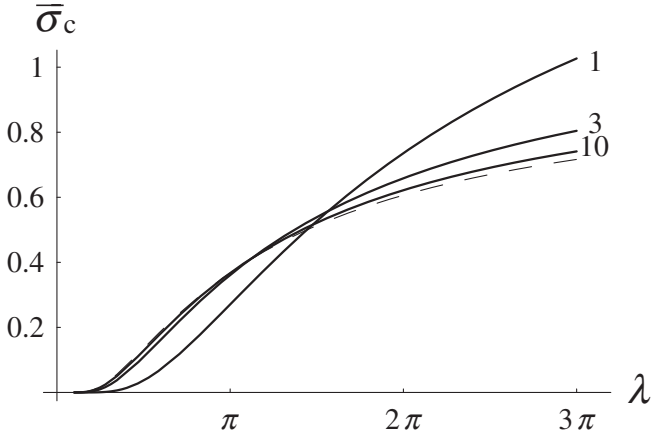

FIG. 5. The dimensionless minimum $\bar{\sigma}_c$ (in units of M) as a function of λ for $T = \mu = 0$. The dashed line represents the $N \to \infty$ result while the continuous lines were produced by the LDE-PMS at order δ. The numbers beside the curves identify the value of N for each case.

The analytical results, Eqs. (3.15) and (3.18), are exact expressions (of course, at this first order of the LDE) following only from the minimization condition, Eq. (3.14), after some algebra. In particular, we emphasize the simple scaling relation obtained between $\bar{\eta}$ and $\bar{\sigma}_c$ in Eq. (3.18), which only depends on N, leading to the result (3.15), and which will prove to be a very good approximation even for the more general case, $T \neq 0$, as we shall see next. Note that this relation is the explicit form, for the case $T = \mu = 0$, of the more general relation, Eq. (3.6), above, namely, $\Sigma_a(\mu = 0, \eta, T = 0) = -\sigma_c/(2N)$.

Actually, there is an simpler, alternative way of deriving the results (3.15), (3.16), (3.17), and (3.18) without using the solution for $\bar{\eta}$ in Eq. (3.13), which will moreover prove useful later on when we shall consider the more complicated situations with $\mu \neq 0$, or typically also if we would consider higher LDE order contributions. That is, instead of using Eq. (3.14) as giving $\bar{\sigma}_c(\bar{\eta})$, we can use it as a substitute for the rather complicated logarithmic dependence $\ln\bar{\eta}/M$ in Eq. (3.12), canceling out, at the same time, the λ dependence, and thus obtaining a very simple linear equation for $\bar{\sigma}_c/\bar{\eta}$ which only depends on N,

$$\frac{\bar{\eta}}{\bar{\sigma}_c} = \left(1 + \frac{1}{2N}\frac{\bar{\sigma}_c}{\bar{\eta}}\right)^{-1}, \tag{3.19}$$

which immediately leads to the results (3.15), (3.16), (3.17), and (3.18). The solution in Eq. (3.13) is useful, however, as it gives $\bar{\eta}$ for any σ_c values, away from the minimum in Eq. (3.14).

B. The $T \neq 0$, $\mu = 0$ case

For the finite temperature but zero chemical potential case, still using Eq. (3.8), the optimized $\bar{\eta}$ is now determined by the solution of the expression

$$\left\{\left[\mathcal{Y}(\eta, T, \mu = 0) + \eta\frac{d}{d\eta}\mathcal{Y}(\eta, T, \mu = 0)\right] \times \left[\eta - \sigma_c + \eta\frac{\lambda}{2\pi N}\mathcal{Y}(\eta, T, \mu = 0)\right]\right\}\Big|_{\eta=\bar{\eta}} = 0. \tag{3.20}$$

The solution coming from the first term in Eq. (3.20) corresponds to the unphysical optimized result, whereas the solution obtained from the second term gives the equivalent of the self-consistent gap equation, (3.12),

$$\bar{\eta}_{\,\delta^1}(\sigma_c, T) = \sigma_c\left[1 + \frac{\lambda}{2\pi N}\mathcal{Y}(\bar{\eta}, T, \mu = 0)\right]^{-1}. \tag{3.21}$$

We could next proceed by numerically solving Eq. (3.21) for $\bar{\eta}$ and substituting it in place of η in Eq. (2.17) (evaluated at $\mu = 0$). Then, by minimizing the effective potential, we would obtain the general behavior of $\bar{\sigma}_c$ as a function of the temperature. The critical temperature for CS restoration would then be determined by the solution of $\bar{\sigma}_c(T = T_c) = 0$ as usual. However, here an explicit analytical result for T_c can also be obtained if we apply the high-temperature approximation to Eq. (2.17), with $\eta/T \ll 1$, and then optimize the resulting expression. The validity of using the high-T approximation before the optimization procedure could be questioned, in principle, since η, at the level of Eq. (2.17), is arbitrary. However, one may easily perform a cross check by performing a numerical PMS application, as described above, without using the high-T expansion. The results we found for T_c from both approaches agree very well with each other, showing that the high-T expansion is valid in a large range, though actually $\bar{\eta}$ and T_c are numerically of the same order of magnitude. A simple reason for this is that the true high-temperature expansion parameter is not η^2/T^2, but rather $7/4[\zeta(3)/(2\pi)^2]\eta^2/T^2 \sim 0.05\eta^2/T^2$, as it is clear from Eq. (3.22) below, so that even if $T_c \sim \eta$ the expansion parameter is still small enough. If we then expand Eq. (2.17) at high temperatures, up to order η^2/T^2, we obtain

$$\begin{aligned}\frac{V_{\mathrm{eff},\delta^1}}{N}(\sigma_c, \eta, T, \mu = 0) = {} & \delta\frac{\sigma_c^2}{2\lambda} - T^2\frac{\pi}{6} - \frac{\eta^2}{2\pi}\left[\ln\left(\frac{Me^{\gamma_E}}{T\pi}\right) - \frac{7\zeta(3)}{4(2\pi)^2}\frac{\eta^2}{T^2}\right] + \delta\frac{\eta(\eta - \sigma_c)}{\pi} \\ & \times\left[\ln\left(\frac{Me^{\gamma_E}}{T\pi}\right) - \frac{7\zeta(3)}{2(2\pi)^2}\frac{\eta^2}{T^2}\right] \\ & + \delta\frac{\lambda}{N}\frac{\eta^2}{(2\pi)^2}\left[\ln^2\left(\frac{Me^{\gamma_E}}{T\pi}\right) - \frac{7\zeta(3)}{(2\pi)^2}\ln\left(\frac{Me^{\gamma_E}}{T\pi}\right)\frac{\eta^2}{T^2} + \mathcal{O}(\eta^4/T^4)\right].\end{aligned} \tag{3.22}$$

Then, setting $\delta = 1$ and applying the PMS, one gets

$$\left[\ln\left(\frac{Me^{\gamma_E}}{T\pi}\right) - \frac{21\zeta(3)}{2(2\pi)^2}\frac{\bar{\eta}^2}{T^2}\right]\left\{\bar{\eta} - \sigma_c + \bar{\eta}\frac{\lambda}{N(2\pi)} \times\left[\ln\left(\frac{Me^{\gamma_E}}{T\pi}\right) - \frac{7\zeta(3)}{2(2\pi)^2}\frac{\bar{\eta}^2}{T^2}\right] + \mathcal{O}(\bar{\eta}^4/T^4)\right\} = 0, \tag{3.23}$$

where, once more, the first term in Eq. (3.23) corresponds to the unphysical (λ independent) solution, while the second term gives

$$\bar{\eta}(\sigma_c, T) = \sigma_c\left\{1 + \frac{\lambda}{N(2\pi)}\left[\ln\left(\frac{Me^{\gamma_E}}{T\pi}\right) - \frac{7\zeta(3)}{2(2\pi)^2}\frac{\bar{\eta}^2}{T^2}\right]\right\}^{-1}, \tag{3.24}$$

whose solution can be expressed in the form

$$\bar{\eta}(\sigma_c, T) = \sigma_c\Bigg\{1 + \frac{\lambda}{N(2\pi)}\Bigg[\ln\left(\frac{Me^{\gamma_E}}{T\pi}\right) - \frac{7\zeta(3)}{2(2\pi)^2}\frac{\sigma_c^2}{T^2} \times\Bigg[1 + \frac{\lambda}{N(2\pi)}\ln\left(\frac{Me^{\gamma_E}}{T\pi}\right)\Bigg]^{-2} + \mathcal{O}(\sigma_c^4/T^4)\Bigg]\Bigg\}^{-1}. \tag{3.25}$$

The result given by Eq. (3.25) is then plugged back into Eq. (3.22) for $\delta = 1$ and the resulting expression is again expanded for $\sigma_c/T \ll 1$ in the high-T approximation. The order of the transition can easily be checked numerically simply by plotting the effective potential for different values of T as shown in Fig. 6.

The result shows that the first order LDE result for finite N predicts a continuous phase transition as in the large-N case. By extremizing the effective potential, at high-T, we obtain a maximum at $\bar{\sigma}_c = 0$ and two minima at

$$\bar{\sigma}_c(T) = \pm\frac{T}{N^2\sqrt{14\pi\zeta(3)\lambda}}\Bigg[2N\pi + \ln\left(\frac{Me^{\gamma_E}}{T\pi}\right)\Bigg]^{3/2} \times\Bigg[-2N\pi + (2N-1)\lambda\ln\left(\frac{Me^{\gamma_E}}{T\pi}\right)\Bigg]^{1/2}. \tag{3.26}$$

Figure 7 shows $\bar{\sigma}_c/M$ given by Eq. (3.26) as a function of T/M, again showing a continuous (second order) phase transition for CS breaking/restoration.

The numerical results illustrated by Figs. 6 and 7 show that the transition is of the second kind and an analytical equation for the critical temperature can be obtained by requiring that the minima vanish at T_c. From Eq. (3.26) one sees that $\bar{\sigma}_c(T = T_c) = 0$ can lead to two possible solutions for T_c. The one coming from

$$\left[2N\pi + \ln\left(\frac{Me^{\gamma_E}}{T_c\pi}\right)\right] = 0 \tag{3.27}$$

can easily be seen as not being able to reproduce the known

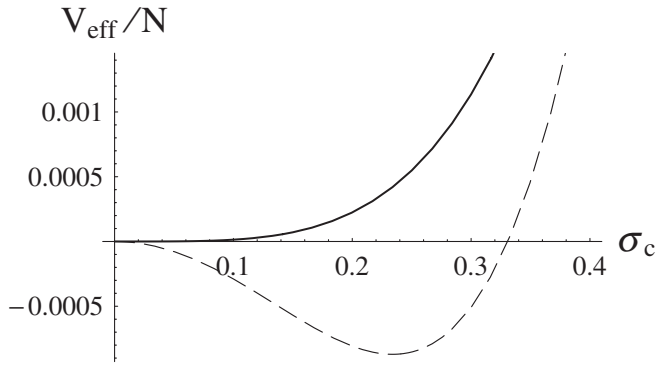

FIG. 6. The effective potential, V_{eff}/N, as a function of σ_c for $\mu = 0$ and $T = 0.170757M$. The parameter values are $\lambda = \pi$ and $N = 3$. The continuous curve, which shows CS restoration, was plotted using the LDE optimized results. The dashed curve, which signals CS breaking, corresponds to the large-N predictions. Both V_{eff}/N and σ_c are in units of M.

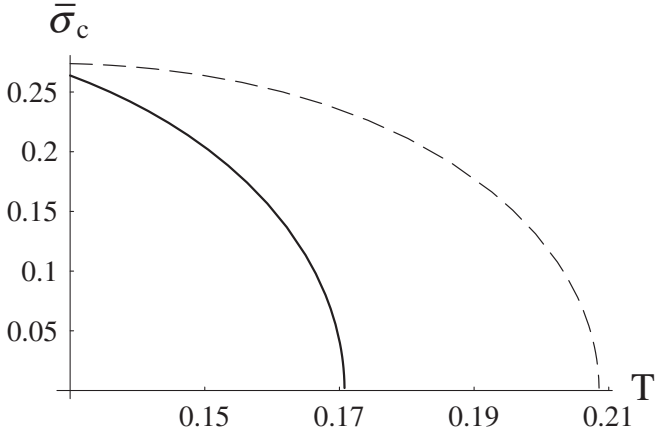

FIG. 7. The nontrivial minimum $\bar{\sigma}_c$ as a function of T for the parameter values $\lambda = \pi$ and $N = 3$. The first order LDE curve (continuous line) displays a continuous phase transition occurring at the critical temperature $T_c = 0.170M$ while the large-N result is $T_c = 0.208M$. Both $\bar{\sigma}_c$ and T are in units of M.

large-N result, when $N \to \infty$, $T_c = M\exp(\gamma_E - \pi/\lambda)/\pi$. However, the other possible solution coming from

$$\left[-2N\pi + (2N-1)\lambda\ln\left(\frac{Me^{\gamma_E}}{\pi T_c}\right)\right] = 0 \tag{3.28}$$

gives for the critical temperature, evaluated at first order in δ, the result

$$T_{c,\delta^1} = M\frac{e^{\gamma_E}}{\pi}\exp\left\{-\frac{\pi}{\lambda[1 - 1/(2N)]}\right\} = M\frac{e^{\gamma_E}}{\pi}\mathcal{F}(\lambda, N), \tag{3.29}$$

with $\mathcal{F}_\lambda(N)$ as given before, by Eq. (3.16). Thus, Eq. (3.29) exactly reproduces the large-N result for $N \to \infty$. The

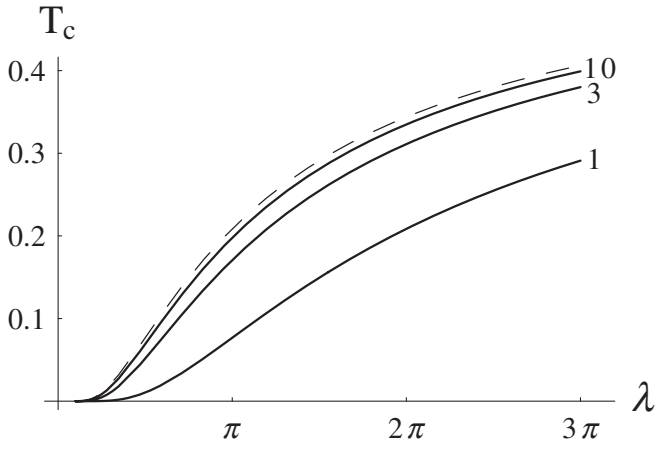

FIG. 8. The dimensionless critical temperature, T_c (in units of M), as a function of λ for $T \neq 0$ and $\mu = 0$. The dashed line represents the $N \to \infty$ result while the continuous lines were produced by the LDE-PMS at order δ. The numbers next to the curves identify the value of N for each case.

results given by this equation are plotted in Fig. 8 as a function of λ for different values of N.

As already mentioned, the critical temperature predicted by Eq. (3.29) coincides, to a very good approximation, with the one observed in the numerical results starting from Eqs. (2.17) and (3.20) without the use of the high-T approximation. We note in Eq. (3.29) the very same scaling relation as the one for $m_F(0)$ at zero temperature, in Eq. (3.18), thus involving a relation that only depends on N. This simple scaling derives, in fact, from the equation for the optimized solution $\bar{\eta}(T)$, where, to obtain the factorized form, Eq. (3.23), we have neglected $\mathcal{O}(1/T^4)$ small terms. Plugging back these neglected terms, and manipulating Eq. (3.23), one easily obtains the relation

$$\sigma_c = \bar{\eta}(T)\left[\left(1-\frac{1}{2N}\right)^{-1} + x^2\frac{\lambda}{\pi}H(\bar{\eta},N)\right], \tag{3.30}$$

where we define for convenience the high-temperature expansion parameter $x \equiv 7/4[\zeta(3)/(2\pi)^2]\bar{\eta}^2/T^2 \sim 0.05\bar{\eta}^2/T^2$, so that $x^2(\lambda/\pi)\bar{\eta}H(\bar{\eta},N)$ defines the remnant part of order $1/T^4$, whose explicit form we do not need to specify. Thus, neglecting these $\mathcal{O}(x^2)$ terms in Eq. (3.30) gives the very same relation between $\bar{\eta}$ and σ_c as at $T=0$ in Eq. (3.18), and, furthermore, Eq. (3.30) is directly related, after some algebra, to the result (3.29) for T_c above. Accordingly, though the simple scaling relation is generally not expected to hold at arbitrary $T \neq 0$, the deviation from this relation is essentially negligible due to the smallness of those $\mathcal{O}(x^2)$ corrections. We shall argue later on, in Sec. III E, that this universal scaling property is expected to remain a good approximation at higher orders of the LDE approximation as well.

The (nonperturbative) LDE result shows that T_c is always smaller (for the realistic finite N case) than the value predicted by the large-N approximation. In light of Landau's theorem for phase transitions in one space dimensions, which predicts $T_c = 0$, our LDE results, including the first $1/N$ corrections, seem to converge to the right direction.

C. The $T = 0$, $\mu \neq 0$ case

As discussed in Ref. [14], this extremum of the phase diagram is very sensitive to the role played by kinklike configurations. However, in the present work, only homogeneous background fields are considered and we are not in a position to compare our results for this part of the phase diagram with the ones provided in that reference. Nevertheless, we are in a position to contribute by computing finite N corrections so that one may, eventually, use the LDE-PMS in conjunction with inhomogeneous background fields to further improve the phase diagram found by the authors of Ref. [14]. The case of zero temperature but finite chemical potential (density) also follows from Eq. (3.8). Using Eqs. (2.18) and (2.19) in Eq. (3.8), we find two situations. In the first, for $\eta > \mu$, the optimized $\bar{\eta}$ is found from the solution

$$\left\{\left[\ln\left(\frac{M}{\eta}\right)-1\right]\left[\eta-\sigma_c+\frac{\lambda\eta}{2\pi N}\ln\left(\frac{M}{\eta}\right)\right]\right\}\Big|_{\eta=\bar{\eta}} = 0. \tag{3.31}$$

For $\eta < \mu$, using the relations (2.18), (2.19), and (2.20) in Eq. (2.17), we obtain that the optimized $\bar{\eta}$ is the solution of

$$\left\{\left[\eta-\sigma_c-\frac{\lambda\eta}{2\pi N}\ln\left(\frac{\mu+\sqrt{\mu^2-\eta^2}}{M}\right)\right]\times\left[-\ln\left(\frac{\mu+\sqrt{\mu^2-\eta^2}}{M}\right)-\frac{\eta^2}{(\eta^2-\mu^2-\mu\sqrt{\mu^2-\eta^2})}\right]-\frac{\lambda\eta}{2\pi N}\right\}\Big|_{\eta=\bar{\eta}} = 0. \tag{3.32}$$

The solution for Eq. (3.31) is exactly the one obtained previously, given by Eq. (3.13). Concerning Eq. (3.32), one can again obtain an analytical solution, by following a reasoning similar to the one done for $T=\mu=0$ leading directly to Eq. (3.19), but with slightly more involved algebra in the present case. Thus, consider the nontrivial minimum $\bar{\sigma}_c$, obtained from $\partial V_{\text{eff}}/\partial\sigma_c = 0$, now for $\mu \neq 0$. From Eq. (2.17) it follows that $\bar{\sigma}_c$ is given by

$$\bar{\sigma}_c = -\frac{\lambda}{\pi}\bar{\eta}\ln\left[\frac{\mu+\sqrt{\mu^2-\bar{\eta}^2}}{M}\right], \tag{3.33}$$

which replaces Eq. (3.14) for $\mu \neq 0$. Now, again, we can use this to simply eliminate the complicated logarithmic dependence $\ln[(\mu+\sqrt{\mu^2-\bar{\eta}^2})/M]$ in Eq. (3.32), thus obtaining, after straightforward algebra, a second order equation for $\bar{\sigma}_c$ as a function of $\bar{\eta}$ and μ, whose explicit solution reads

$$\bar{\sigma}_c = \frac{1}{2}\frac{\bar{\eta}}{1-1/(2N)}\left[1+G(\lambda,\bar{\eta},\mu,N) + \sqrt{[1-G(\lambda,\bar{\eta},\mu,N)]^2-\frac{2}{N}\left(1-\frac{1}{2N}\right)\frac{\lambda^2}{\pi^2}}\right], \tag{3.34}$$

where

$$G(\lambda,\bar{\eta},\mu,N) \equiv \frac{\lambda}{\pi}\left(1-\frac{1}{2N}\right)\left(1-\frac{\mu}{\sqrt{\mu^2-\bar{\eta}^2}}\right) \tag{3.35}$$

contains the μ dependence. The relation (3.34) is the appropriate generalization, for $\mu \neq 0$, of the simple scaling relation obtained at $T=\mu=0$ in Eq. (3.18). We have eliminated the other possible solution for $\bar{\sigma}_c$ [namely, with $\sqrt{\cdots} \to -\sqrt{\cdots}$ in Eq. (3.34)], by noting that, for $\lambda \to 0$, Eq. (3.34) correctly reproduces the simpler scaling relation in (3.18), while the other solution would give $\bar{\sigma}_c \to 0$.[2] It

[2]The leading order large N relation $\bar{\sigma}_c = \bar{\eta}$ is also consistently reproduced for $N \to \infty$ in Eq. (3.34).

will also prove useful to expand Eq. (3.34) in powers of λ:

$$\bar{\sigma}_c \sim \frac{\bar{\eta}}{1-1/(2N)}\Big[1-\frac{1}{2N}\Big(1-\frac{1}{2N}\Big)\Big(\frac{\lambda}{\pi}\Big)^2 + \frac{1}{2N}\Big(1-\frac{1}{2N}\Big)^2\Big(1-\frac{\mu}{\sqrt{\mu^2-\bar{\eta}^2}}\Big)\Big(\frac{\lambda}{\pi}\Big)^3 + \mathcal{O}\Big(\frac{\lambda}{\pi}\Big)^4\Big], \tag{3.36}$$

which should thus be valid for moderate values of λ/π. This immediately shows that the corrections due to $\mu \neq 0$ to the simple scaling obtained previously for $T = \mu = 0$ in Eq. (3.18) are actually suppressed by $\mathcal{O}(\lambda^2/(\pi^2 N))$; moreover, the μ dependence enters only at the next order, $(\lambda/\pi)^3$. These properties are somewhat analogous to the case of the $T \neq 0$ ($\mu = 0$) corrections to the scaling in Eq. (3.30), which are also suppressed by the small high-temperature expansion parameter. We shall come back to the important consequences of these relations for the general case T, $\mu \neq 0$ in the next subsections.

Next, we extract the critical chemical potential, μ_c, and, as in the large-N problem [22,23], we can check that a first order transition also occurs. To this aim we first calculate the effective potential at the value σ_c given by Eq. (3.15), where the relevant expression is given by $V_{\text{eff}}(\sigma_c)$ for $\mu < \eta$. After some algebra, many terms cancel out so that we simply obtain

$$V_{\text{eff}}^{\delta^{(1)}}(\sigma_c = \bar{\sigma}_c, \eta = \bar{\eta}) = -\frac{\bar{\eta}_{\delta^1}^2}{4\pi}, \tag{3.37}$$

i.e., the same expression as the leading order $N \to \infty$ one, but with the appropriate fermion mass at first order in δ, and $\bar{\eta}_{\delta^1}$ given by Eq. (3.18). This now has to be compared with the value of V_{eff} for $\mu \neq 0$ but with $\eta = 0$, which is simply obtained from Eq. (2.17) as

$$V_{\text{eff}}^{\delta^{(1)}}(\sigma_c = \eta = 0, \mu) = -\frac{\mu^2}{2\pi}\Big(1-\frac{\lambda}{2\pi N}\Big), \tag{3.38}$$

so that we can deduce an analytic expression for the critical density μ_c,

$$\mu_{c,\delta^1} = \frac{\bar{\eta}_{\delta^1}}{\sqrt{2}}\Big(1-\frac{\lambda}{2\pi N}\Big)^{-1/2}, \tag{3.39}$$

valid at this first order in δ. The appearance of a pole in Eq. (3.39) for $\lambda = 2\pi N$ is an artifact of our first order in δ approximation and thus probably not physically relevant. The point is that going to higher orders in the expansion in δ will also bring different corrections of the same order in powers of $1/N$, if expanded. Thus, we could, for example, limit ourselves in this analysis to the first $1/N$ order in this expansion, since complete $1/N^2$ corrections are not included at the order in δ we are considering. Seen this way, we could also expand Eq. (3.39) in powers of $1/N$,

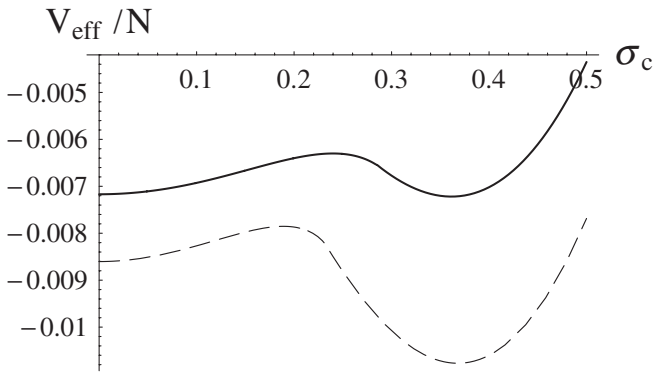

FIG. 9. Large-N (dashed line) and first order LDE (continuous line) results for the effective potential, V_{eff}/N. The parameter values are $N = 3$, $\lambda = \pi$, and $T = 0$. The effective potential has been evaluated at the (first order) LDE critical value $\mu_c = 0.232M$ for which the large-N approximation still predicts CSB. Both V_{eff}/N and μ are in units of M.

$$\mu_{c,\delta^1,1/N} = \frac{M}{\sqrt{2}}\exp(-\pi/\lambda)\Big[1-\frac{\pi}{2N\lambda}+\frac{\lambda}{4\pi N} + \mathcal{O}(1/N^2)\Big], \tag{3.40}$$

which then exhibits no pole.

We also proceed numerically to obtain the solution from (3.32) and subsequent values of μ_c, in order to have a useful crosscheck of the more complicated most general case with both T and μ finite, where analytical expressions are not available. An example for fixed values of N and λ is presented in Fig. 9, which shows the effective potential as a

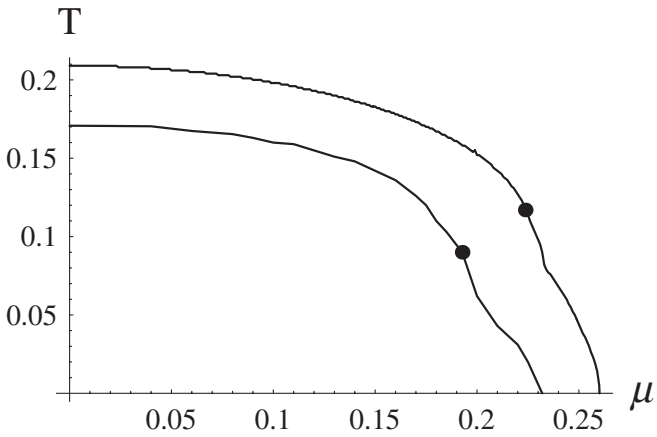

FIG. 10. Large-N (outermost line) and LDE (innermost line) phase diagrams. The parameter values are $N = 3$ and $\lambda = \pi$. The dots represent the tricritical points. The large-N result for the tricritical point is $P_{\text{tc},N\to\infty} = (T_{\text{tc}}, \mu_{\text{tc}}) = (0.117, 0.224)$ while the LDE approximation gives $P_{\text{tc},\delta^1} \simeq (T_{\text{tc}}, \mu_{\text{tc}})_{\delta^1} = (0.091, 0.192)$. In both cases, the lines above the tricritical point represent second order phase transitions while the ones situated below represent first order transitions. All quantities are given in units of M.

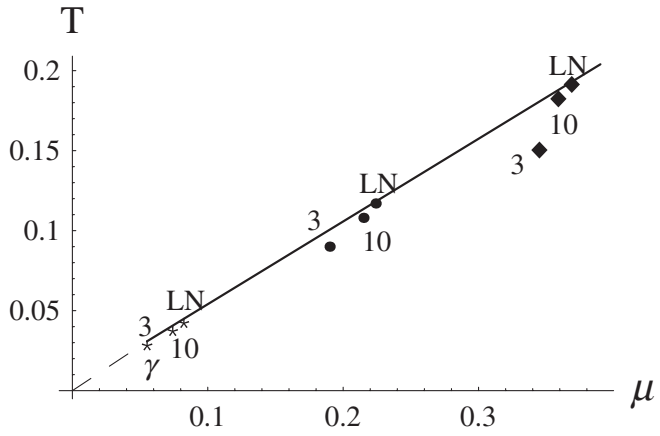

FIG. 11. The tricritical points $P_t = (T_{tc}, \mu_{tc})$, in units of M, for different values of λ and N. The stars represent $\lambda = \pi/2$, the dots $\lambda = \pi$, and the diamonds $\lambda = 2\pi$. The corresponding values of N are directly specified by the numbers on the graph. The angle γ represents the quantity T_{tc}/μ_{tc} as discussed in the text.

function of σ_c. The condition that the minimum of the potential at $\bar{\sigma}_c = 0$ be the same as the one at $\bar{\sigma}_c = m_F$, at some $\mu = \mu_c$, leads to the result $\mu_{c,\delta^1} \simeq 0.232M$, in the first order of the LDE, which should be compared with the large-N result, $\mu_{c,N\to\infty} \simeq 0.260M$.

D. The $T \neq 0$, $\mu \neq 0$ case

We now arrive at the point of analyzing the complete LDE phase diagram, at order δ. Because of the lack of possible fully analytical solutions in this general case, we use numerical routines to determine curves of both the second order and first order phase transitions and their point of intersection which then defines the tricritical point. In Fig. 10 we show the large-N result compared to the LDE first order result. It can be seen that, in the LDE nonperturbative approach, the region for chiral symmetry breaking (CSB) is diminished in an appreciable way. In units of M, the LDE result for the tricritical point, with $N = 3$ and $\lambda = \pi$, is $P_{tc,\delta^1} = (T_{tc}, \mu_{tc})_{\delta^1} = (0.091, 0.192)$, while the large-$N$ approximation gives $P_{tc,N\to\infty} = (T_{tc}, \mu_{tc}) = (0.117, 0.224)$.

It is worth noting how the LDE tricritical point falls, approximately, over a line joining the large-N result and the origin. This remarkable result is shown in Fig. 11 which shows P_{tc} for $\lambda = \pi/2, \pi, 2\pi$ and $N = 3, 10$, and $N \to \infty$ (LN). A deviation of about 9% is observed only for large values of the ratio λ/N (e.g., $2\pi/3$). For ratios close to unity, the deviation is very small (about 3%).

E. Generality of scaling for the LDE results

For moderate values of λ/N, we thus note the approximate invariance, up to very small corrections in the LDE finite N case, of the ratio T_{tc}/μ_{tc} that defines the angle γ,

$$\tan\gamma = \frac{T_{tc}}{\mu_{tc}} \simeq 0.523. \tag{3.41}$$

All our results show that this ratio remains, to a good approximation, largely independent of both N and λ. As already discussed, this strongly suggests postulating a very simple (but approximate) result for the predictions of the tricritical points and for all other dimensionful quantities obtained for the GN model within the LDE. The result (3.41) indicates that T_{tc} and μ_{tc}, as a function of N and λ, to a good approximation in the relevant range, scale according to

$$T_{tc}(\lambda, N) \simeq c\, g(\lambda, N) M, \tag{3.42}$$

$$\mu_{tc}(\lambda, N) \simeq g(\lambda, N) M, \tag{3.43}$$

where $c = \tan\gamma$ and $g(\lambda, N)$ is a function of the parameters λ and N. At the first LDE order, we have obtained explicitly $g(\lambda, N) = \mathcal{F}(\lambda, N)$, where $\mathcal{F}(N)$ is given by Eq. (3.16), up to very small corrections in the $T \neq 0$ ($\mu = 0$) case. For the case $\mu \neq 0$ ($T = 0$) we see that the approximation is valid only for $\lambda \leq \pi$, approximately, which is easily understood by examining the approximate expanded form, Eq. (3.36), of the relation, Eq. (3.34). As anticipated, one can see that the corrections for $\mu \neq 0$ to the simple scaling relation (3.18), strictly valid for $T = \mu = 0$ only, are moderate as long as λ is not too large, which essentially remains true also for the more general case $T \neq 0$ and $\mu \neq 0$.

Interestingly, the actual result for the tricritical points, if compared with the large-N result, which, in units of $m_F(0)$, is given by $P_{tc} = (T_{tc}, \mu_{tc}) = (0.318, 0.608)$ [15], is of the form

$$P_{tc} = (T_{tc}, \mu_{tc}) \simeq (0.318, 0.608)\, \bar{\eta}_{\delta^1}(\bar{\sigma}_c), \tag{3.44}$$

where $\bar{\eta}_{\delta^1} = \mathcal{F}(\lambda, N) M$. The numerical deviations from the above result are very small (less than 5%) for $\lambda/N < 1.3$.

The result (3.44) together with our previous results obtained within the first order in the LDE, Eqs. (3.15), (3.29), and (3.39), respectively, for the fermion mass ($\bar{\sigma}_c$), critical temperature (T_c), and critical chemical potential (μ_c), show the same approximate scaling as given in terms of the optimized LDE quantity $\bar{\eta}_{\delta^1}$. Also, as we have already seen previously, in the large-N limit, $\bar{\eta}_{\delta^1}(\bar{\sigma}_c) \to m_F(0)$ and all our LDE results correctly reproduce the standard large-N results.

The reason why most of our results (except perhaps for the somewhat extreme case $T = 0$, $\mu \neq 0$) exhibit approximately universal scaling properties as a function of $\bar{\eta}$, to a very good approximation, is well understood at the first LDE order, as explained in the previous subsections. On more general grounds, in writing the interpolated Lagrangian density, Eq. (2.3), an explicitly dimensionful (mass) parameter, η, is introduced in the originally mass-

less model where there is no other dimensionful parameter. Thus, from a simple dimensional analysis, clearly all physical quantities should scale with η, or actually $\bar{\eta}$ derived from the optimization procedure.[3] More precisely, at first LDE order, and $T = \mu = 0$, we obtain the exact simple relation, Eq. (3.18), between $\bar{\eta}$ and σ_c, which only depends on N. More generally, in terms of the basic scale of the model, say $\bar{\Lambda} \equiv Me^{-\pi/\lambda}$ in the $\overline{\text{MS}}$ renormalization scheme, truly nonperturbative results are expected to give, for the ratio of the relevant quantities $m_F/\bar{\Lambda}$, $T_c/\bar{\Lambda}$, and $\mu_c/\bar{\Lambda}$, some specific dimensionless coefficients depending only on N. *A priori*, there is no reason why these coefficients should be exactly the same for the three quantities. In contrast, on purely perturbative grounds, for $T \neq 0$ and $\mu \neq 0$ we expect, at finite LDE order, to obtain after optimization more complicated scaling relations, i.e., not only with different coefficients for the three relevant quantities, but also with such coefficients being some nontrivial (dimensionless) functions of T, μ, σ_c, λ, and N. Indeed, an explicit example that this is the case already at first LDE order is illustrated by the relations, Eq. (3.30), for $T \neq 0$, and Eq. (3.34) for $\mu \neq 0$. Both relations strictly depend on λ and T (or, respectively, μ). However, we have seen that, quite remarkably, this extra dependence upon the coupling is quite suppressed, in such a way that the fermion mass m_F, critical temperature T_c, and even μ_c have, to a very good approximation, identical scaling factors which only depend on N. Moreover, we have shown that, in the $T \neq 0$ ($\mu = 0$) case, this result is not a numerical accident but can be well understood analytically by noting that the corrections to this universal scaling are intrinsically quite negligible. Even in the most general case when both $T \neq 0$ and $\mu \neq 0$, the results for the tricritical point happen in a regime where the simple scaling relation appears to still be a good approximation. The only exception is the somewhat extreme case when $T = 0$ and $\mu \neq 0$: in this case, if λ is sufficiently large, the appropriate generalization given analytically by Eq. (3.34) leads to substantial deviations from the simple scaling relation for $T = \mu = 0$ in Eq. (3.18).

We believe, in fact, that this trend generalizes as well to arbitrary higher orders of the LDE expansion, as we shall argue heuristically next. To examine what is happening at higher LDE orders, let us first consider the $T = \mu = 0$ case. It is simpler to generalize the reasoning used to obtain Eq. (3.19) at first δ order, i.e. using the solution σ_c of Eq. (3.14) to substitute the logarithmic dependence $\ln(\bar{\eta}/M)$ into the (optimization) equation defining $\bar{\eta}$, which thus generalizes Eq. (3.12) at higher orders. In this way the latter will be a simpler, purely algebraic equation, for the (only) parameter $\sigma_c/\bar{\eta}$, in terms of the remaining parameters, the coupling λ and N. More precisely, at higher LDE orders, from general arguments the effective potential will have additional perturbative terms of the generic form

$$\sim \sum_{k\geq 2} (\eta_*)^2 \delta^k \left(\frac{\lambda}{2\pi}\right)^k \left[c_{\text{LL}}(N) \ln^{k+1} \frac{\eta_*}{M} + c_{\text{NLL}}(N) \ln^k \frac{\eta_*}{M} + \cdots \right] \tag{3.45}$$

powers of $\ln(\eta_*/M)$. The corresponding coefficients can be calculated from the relevant Feynman graphs. Next, performing the LDE to some given order and taking the limit $\delta \to 1$, etc., the resulting dependence upon σ_c and η is much more involved than at first order, so that one obtains from the CS breaking condition a nonlinear relation for σ_c, generalizing Eq. (3.18), and as well for the optimized $\bar{\eta}$ solution, Eq. (3.12). Nevertheless, it is clear that these two relations can be used e.g. to eliminate the logarithmic dependence $\ln\bar{\eta}/M$, thus obtaining a polynomial equation for $\sigma_c/\bar{\eta}$, which only depends on N and λ. Actually, if we were able to resum this LDE series to all orders, we would certainly expect that the only dependence on the coupling λ in all physical quantities would be entirely included in terms of the basic dimensionful scale of the model e.g. in the $\overline{\text{MS}}$ scheme: $\Lambda_{\overline{\text{MS}}} \equiv Me^{-\pi/\lambda}$. However, at finite LDE orders, the optimization generally defines a rather complicated dependence on λ for $\bar{\eta}$. But we have checked explicitly at the next (δ^2) order that this induces relatively small deviations from the first order scaling relation in Eq. (3.18) [upon assuming, obviously, that the unknown coefficients c_i appearing in Eq. (3.45) take generic values of $\mathcal{O}(1)$]. Next, we saw that the $T \neq 0$ result gives, at this LDE order, a very small correction to the scaling relation existing for $T = 0$. For $\mu \neq 0$, a deviation from this simple scaling is predicted by Eq. (3.34); however, it remains numerically moderate up to relatively large values of the coupling λ. Now, since, as we just examined, the $T = 0$ scaling properties are expected to generalize at higher LDE orders, and the LDE generally converges quite rapidly, we can expect that the higher order modifications for T, $\mu \neq 0$ to these first LDE order scaling properties should remain small corrections.

IV. COMPARING THE LDE AND THE $1/N$ RESULTS

Let us compare, in this section, the LDE leading order results with the ones given by the $1/N$ approximation at leading order (LO) as well as next-to-leading order. As

[3]Note that, though at first the interpolation procedure done in Eq. (2.3) seems to explicitly break the discrete chiral symmetry of the model, η is initially an undetermined parameter. The introduction of the auxiliary field σ just makes the optimized η a function of the background scalar field σ_c. After optimization $\bar{\eta}(\sigma_c) \sim \sigma_c$, so chiral symmetry breaking and restoration have the same interpretation as in the original (noninterpolated) GN model. It is a nonvanishing value for the minimum of the σ field effective potential, $\langle\sigma\rangle_0 = \bar{\sigma}_c \neq 0$, that still signals the breakdown of chiral symmetry, and $\bar{\eta}(\bar{\sigma}_c) \sim \bar{\sigma}_c$ provides the scale for all physical quantities derived.

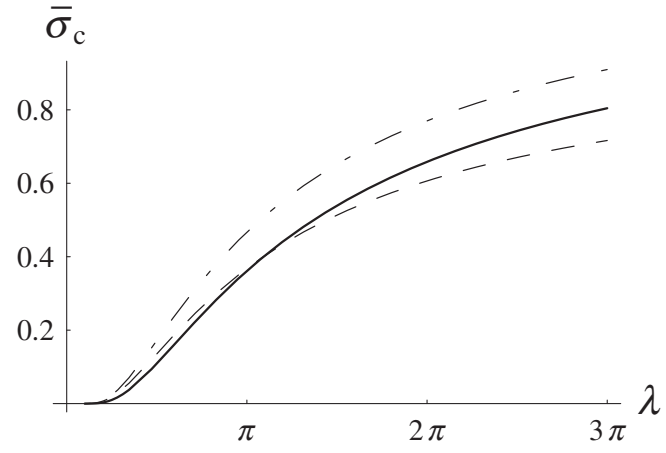

FIG. 12. The fermionic mass $m_F(0) = \bar{\sigma}_c$, in units of M, plotted as a function of λ for $N = 3$, $T = 0$, and $\mu = 0$. The dashed line represents the $1/N$ result at leading order, the dot-dashed line represents the $1/N$ result at next-to-leading order, and the continuous line is the first order LDE result.

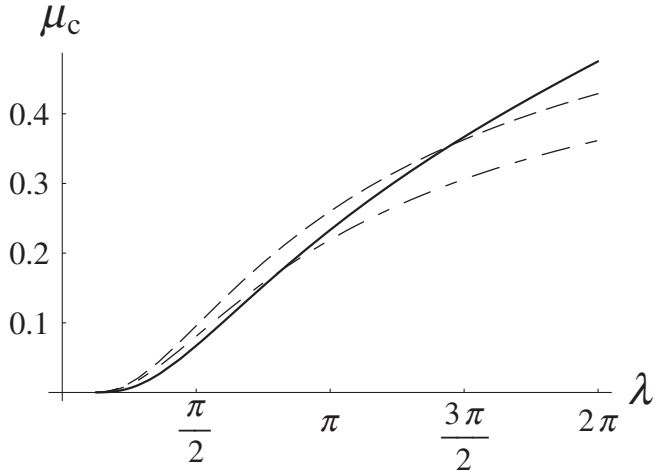

FIG. 13. The critical chemical potential μ_c in units of M, plotted as a function of λ for $N = 3$ and $T = 0$. The dashed line represents the $1/N$ result at leading order, the dot-dashed line represents the $1/N$ result at next-to-leading order, and the continuous line is the first order LDE result.

already pointed out, the effective potential, at $T = 0$ and $\mu = 0$, for the 2d Gross-Neveu model to the NLO was first evaluated by Root [35]. The NLO correction to the fermionic mass, at $T = \mu = 0$, was explicitly evaluated by Forgács, Niedermayer, and Weisz [38]. Using a combination of the thermodynamic Bethe ansatz and the $1/N$ effective potential at $T = \mu = 0$, Chodos and Minakata [39] were able to obtain the NLO correction for μ_c. Recently, the authors in Ref. [13] computed the complete NLO in the $1/N$ expansion for the effective potential at $T \neq 0$ and $\mu = 0$, performing a detailed numerical analysis of their results. They also exhibited, in detail, a number of nontrivial properties, in particular, for the expected behavior at high temperature, but because of the appearance of a Landau pole near the $T \sim T_c$ regime, they do not conclude with a well-defined value of T_c from the full $1/N$ calculation. It is thus difficult to compare our numerical LDE estimates of T_c with their numerical results.

Next, we emphasize that, as far as we know, there are no $1/N$ NLO results for the case $T \neq 0$ and $\mu \neq 0$; thus, there are no results for the tricritical points beyond the large-N approximation. For comparison purposes, let us use our notations and conventions to present the only two available analytical results.

For the case $T = \mu = 0$, Ref. [38] gives[4]

$$\bar{\sigma}_c^{1/N,\mathrm{NLO}}(0) = M \exp(-\pi/\lambda)\left[1 + \frac{1}{N}(2\ln 2 - \gamma_E)\right]. \tag{4.1}$$

[4]In our comparison with the exact $1/N$ result of the fermion mass as given in Ref. [38], we should be cautious to *remove* from their expression a term, $M\exp(-\pi/\lambda)/N$, since our scheme is such that our reference scale is $M\exp(-\pi/\lambda)$, rather than the full $\Lambda_{\overline{\mathrm{MS}}}$ expression of [38].

Figure 12 shows the LDE fermionic mass at $T = 0 = \mu$, $\bar{\sigma}_c = M\mathcal{F}(\lambda, N)/[1 - 1/(2N)]$, as a function of λ for $N = 3$. The same figure shows the $1/N$ results at LO, given by Eq. (3.17), and at NLO, given by Eq. (4.1).

For the case $T = 0$, $\mu \neq 0$, Ref. [39] gives

$$\mu_c^{1/N,\mathrm{NLO}} = \frac{M}{\sqrt{2}} \exp(-\pi/\lambda)\left(1 - \frac{0.47}{N}\right). \tag{4.2}$$

Figure 13 shows the LDE critical chemical potential at $T = 0$, $\mu_c = M/\sqrt{2}\mathcal{F}(\lambda, N)$, as a function of λ for $N = 3$. The same figure shows the $1/N$ results at NLO, given by Eq. (4.2), and LO, given by the $N \to \infty$ of Eq. (4.2). As we have emphasized in the text, the LDE results for this case are valid only up to $\lambda \sim \pi$. Apart from that, this is the case where kinklike configurations start to play a major role, so any quantitative results must be interpreted with due care [14].

V. CONCLUSIONS

The analytical nonperturbative technique known as the LDE has been applied to the two-dimensional Gross-Neveu model effective potential at finite temperature and chemical potential. Following the prescription suggested in Ref. [27], we have shown that, within the large-N limit, the LDE exactly agrees with the $1/N$ LO exact result for any values of T or μ. Having established this reliability, we have considered the first finite N correction that already appears at the first nontrivial order. The variational optimization procedure has produced interesting results that turned out to be possible to be cast into analytical form. A careful analysis of our numerical and analytical optimized results has led us to write down five simple relations, which take into account finite N corrections, concerning the

$T = 0 = \mu$ fermionic mass ($\bar{\sigma}_c$), μ_c (at $T = 0$), T_c (at $\mu = 0$), and the tricritical points ($T_{t,c}$, $\mu_{t,c}$). As we have discussed, four of these quantities essentially scale, to a very good approximation, with the LDE optimized mass scale at $T = 0 = \mu$ given by $\bar{\eta}_{\delta^1}/M = \mathcal{F}(\lambda, N)$, with $\mathcal{F}(\lambda, N)$ defined by Eq. (3.16), $\bar{\eta}$ being the only dimensionful quantity present in the interpolated Lagrangian density. The only exception is the case of μ_c for $T = 0$ where, for large enough coupling λ, we obtained substantial deviation from the simple scaling, with an explicit expression of its dependence on λ. However, as already mentioned, we believe our results are not faithful in the small T and large μ part of the phase diagram, which is most substantially affected by inhomogeneous backgrounds, as shown at leading $1/N$ order in Ref. [14]. The basic reasons for the approximately very good validity of the universal scaling relations, at the first LDE order, were identified and understood, as explained in some detail in Sec. III. Moreover, we argued that this quasiuniversality of scaling is expected to hold also at arbitrary higher orders of the LDE. At $T \neq 0$ and $\mu \neq 0$, our main results concern the evaluation of the phase diagram, containing finite N corrections that, as far as we know, have not been carried out before. Comparing our perturbative type of evaluation with the ones performed in Refs. [13,38,39], for example, one may notice some of the LDE advantages. Namely, it automatically introduces an infrared cutoff that makes completely perturbative evaluations possible. At the same time, at each (perturbative) order, one has just a few Feynman graphs to evaluate as compared to the traditional nonperturbative methods, such as the $1/N$ approximation. In particular, this advantage of the LDE procedure means that the renormalization program can be easily implemented. Now, to proceed beyond the first LDE order, as far as the $T \neq 0$, $\mu = 0$ case is concerned, it could be interesting, in principle, to exploit those full $1/N$ results of Ref. [13], by reexpanding them in ordinary perturbation theory in the coupling λ, and then proceeding with the LDE procedure as outlined in Sec. II. However, after definite efforts to do this, it proves to be of very little use for our purposes, simply because beyond the first LDE order one can obtain these results only in purely numerical form. To perform the LDE, we necessarily need to at least have the analytical dependence upon the coupling λ and fermion mass to be able to perform the interpolation as described in Eq. (2.3). Moreover, even at first order, it is very difficult to compare our results with theirs, due to the different momenta routing used, resulting in their much more involved expressions of the T-dependent contributions, in particular (note, however, that this alternative routing is the only possible one beyond the first order). More generally, at the first LDE order investigated here, we cannot expect to get very close to the exact $1/N$ results, but, at the same time, we expect the LDE to converge faster and incorporate terms beyond the $1/N$ at higher orders, as discussed before.

Speculating on the expected behavior at higher LDE orders, the occurrence of a Landau pole in the complete $1/N$ results found by the authors of Ref. [13], therefore invalidating *a priori* an unambiguous determination of a T_c value, deserves some general comments. Accordingly, it is useful to recall how the Landau pole emerges in the construction of Ref. [13]: in very rough terms, at finite T a pole can occur in the dressed propagator of the σ field for some value of the T-dependent effective fermion mass, $m_F(T)$, because the latter decreases as T increases from zero, eventually reaching $m_F(T_c) = 0$ at critical temperature.[5]

Now, it is interesting to note that the LDE will avoid this Landau pole problem, in a rather trivial way: by construction, the LDE stops at *finite* orders, where there cannot be a pole, while a Landau pole is relevant only when considering a resummed perturbative series. Moreover, let us assume that one could manage to resum the LDE perturbative series to all orders, in some approximation (which can be done explicitly e.g. for the GN mass gap [24,25] at order $1/N$, using the LDE together with renormalization group properties): one would thus obtain a resummed expression possibly exhibiting a pole at a critical mass value, but even in such a case, the optimization prescription used in the LDE construction will escape this pole, i.e. the optimization ''freezes out'' the mass at a value which generally cannot coincide with a possible Landau pole value.

Although convergence properties cannot be accessed in the first nontrivial order, the fact that our T_c is, in accordance with Landau's theorem, smaller than the LO large N result gives further support to the method. However, a deeper discussion about convergence is beyond the scope of the present work due to the technical difficulties in evaluating, at $T \neq 0$ and $\mu \neq 0$, some of the three-loop graphs shown in Fig. 2. We recall that the LDE-PMS convergence properties in critical theories have been analyzed, by the present authors, in connection with homogeneous Bose-Einstein condensates [9]. We intend to extend the present work by considering the order-δ^2 three-loop graphs that will bring the first $1/N^2$ corrections. This will help us to gauge convergence properties, the effects of the $1/N^2$ terms, as well as the eventual generalization of the universal scaling relations between the critical and tricritical quantities with the LDE optimized mass scale.

ACKNOWLEDGMENTS

M. B. P. and R. O. R. are partially supported by CNPq-Brazil. M. B. P. thanks the Laboratoire de Physique Théorique et Astroparticules (Université de Montpellier II) for a CNRS guest grant, and R. O. R. also acknowledges partial support from FAPERJ.

[5]Note, in contrast, that this Landau pole is harmless at $T = 0$, because in the corresponding exact $1/N$ calculation of the mass gap (see e.g. [38,40]), this pole actually cannot be reached for any consistent value of the mass gap.

APPENDIX A: SUMMING MATSUBARA FREQUENCIES AND RELATED FORMULAS

The integrals encountered in Feynman's graphs are performed, as usual, at finite temperature and density with the substitution rules $p_0 \to i(\omega_n - i\mu)$, where μ is the chemical potential and $\omega_n = (2n+1)\pi T$, $n = 0, \pm 1, \pm 2, \ldots$, are the Matsubara frequencies for fermions. We sum over the Matsubara frequencies with standard contour integration techniques, regularize the remaining (Euclidean) momentum integrals with dimensional regularization, and carry out the renormalization in the $\overline{\text{MS}}$ scheme. In general, momentum integrals of functions $f(p_0, |\mathbf{p}|)$ are replaced by (see Ref. [41])

$$\int \frac{d^2p}{(2\pi)^2} f(p_0, |\mathbf{p}|) \to iT \sum\!\!\!\!\!\!\int f[i(\omega_n - i\mu), |\mathbf{p}|] = iT \sum_n \int \frac{dp}{(2\pi)} f[i(\omega_n - i\mu), |\mathbf{p}|].$$

For the divergent, zero temperature contributions, dimensional regularization is carried out in dimensions $d = 1 - 2\epsilon$ and in the $\overline{\text{MS}}$ scheme, in which case the momentum integrals are written as

$$\int \frac{dp}{(2\pi)} \to \int_p = \left(\frac{e^{\gamma_E} M^2}{4\pi}\right)^{\epsilon} \int \frac{d^d p}{(2\pi)^d},$$

where M is an arbitrary mass scale and $\gamma_E \simeq 0.5772$ is the Euler-Mascheroni constant.

The Matsubara sums which are relevant for the different integrals considered in Sec. II can be derived as (see e.g. [41])

$$T \sum_{n=-\infty}^{+\infty} \ln[(\omega_n - i\mu)^2 + \omega^2(\mathbf{p})] = \omega(\mathbf{p}) + T \ln\{1 + e^{-[\omega(\mathbf{p})+\mu]/T}\} + T \ln\{1 + e^{-[\omega(\mathbf{p})-\mu]/T}\}, \tag{A1}$$

$$T \sum_{n=-\infty}^{+\infty} \frac{1}{(\omega_n - i\mu)^2 + \omega^2(\mathbf{p})} = \frac{1}{2\omega(\mathbf{p})} \left\{1 - \frac{1}{e^{[\omega(\mathbf{p})+\mu]/T} + 1} - \frac{1}{e^{[\omega(\mathbf{p})-\mu]/T} + 1}\right\}, \tag{A2}$$

$$T \sum_{n=-\infty}^{+\infty} \frac{\omega_n - i\mu}{(\omega_n - i\mu)^2 + \omega^2(\mathbf{p})} = \frac{i}{2} \frac{\sinh(\mu/T)}{\cosh(\mu/T) + \cosh(\omega(\mathbf{p})/T)}, \tag{A3}$$

where $\omega^2(\mathbf{p}) = \mathbf{p}^2 + \eta^2$.

APPENDIX B: RENORMALIZATION OF THE LDE EFFECTIVE POTENTIAL

For renormalization purposes, we can also add to the Gross-Neveu model a counterterm Lagrangian density, $\mathcal{L}_{\text{ct}}$, whose most general form can be expressed as

$$\mathcal{L}_{\text{ct}} = \bar{\psi}_k (iA\partial\!\!\!/)\psi_k - B\sigma\bar{\psi}_k\psi_k - C\frac{\sigma^2 N}{2\lambda} + D\bar{\psi}_k\psi_k + E\sigma + X, \tag{B1}$$

where A, B, C, D, E, and X are renormalization counterterms with the latter representing the zero point energy subtraction. We give here some details on the renormalization procedure for the effective potential of the interpolated model (2.5). First, let us consider the nonrenormalized result for the effective potential in the large-N approximation, which from Eq. (2.8) is given by

$$\frac{V_{\text{eff},\delta^1}}{N}(\sigma_c, \eta_*, N \to \infty) = \delta\frac{\sigma_c^2}{2\lambda} - \frac{1}{2\pi}\left\{\eta_*^2\left[\frac{1}{\epsilon} + \frac{1}{2} + \ln\left(\frac{M}{\eta_*}\right)\right] + 2T^2 I_1\left(\frac{\eta_*}{T}, \frac{\mu}{T}\right)\right\}. \tag{B2}$$

Going beyond large N one must add the order-δ term, Eq. (2.11),

$$V^{(a)}_{\text{eff},\delta^1}(\eta_*) = -i\frac{1}{2}\int \frac{d^2p}{(2\pi)^2}\,\text{tr}\left[\frac{\Sigma_a(\eta_*)}{p\!\!\!/ - \eta_* + i\epsilon}\right], \tag{B3}$$

where Σ_a is the term 3c in Fig. 14,

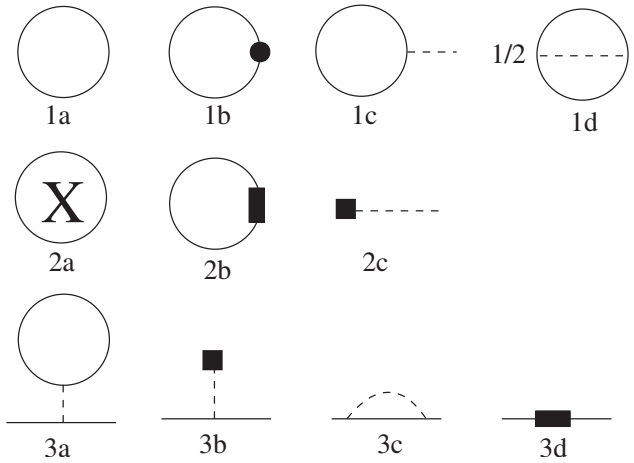

FIG. 14. Feynman diagrams contributing to the effective potential up to order δ. Diagrams 1a, 1b, 1c, and 1d are the LDE ultraviolet divergent contributions. Diagram 1d has a symmetry factor 1/2. Diagram 2a represents the counterterm corresponding to the zero point energy subtraction. Diagram 2b is constructed with the counterterm (3d) which renormalizes the exchange self-energy (3c). The linear counterterm 2c can be obtained by renormalizing (with 3b) the direct self-energy term, 3a.

$$\Sigma_a(\eta_*) = -\delta\left(\frac{\lambda}{N}\right) i \int \frac{d^2q}{(2\pi)^2} \frac{1}{\not{q} - \eta_* + i\epsilon}. \tag{B4}$$

It is worth noting that the relative simplicity of our final result, Eq. (2.13), for this two-loop graph is largely due to the appropriate choice of momenta routing, allowing us to factorize the result into (squared) one-loop contributions. We checked explicitly that it is strictly equivalent to another momenta routing choice in the literature [13,35], more appropriate when considering higher order contributions but which at this two-loop level would result in much more involved intermediate expressions.

As it has been shown [6,24], the standard $\overline{\text{MS}}$ renormalization procedure and the LDE commute with each other, so that one may perform the LDE before renormalization (thus introducing extra δ-dependent counterterms) or, alternatively, directly on renormalized quantities. We shall rather follow here the first approach which may be more illustrative for our purpose. An explicit evaluation of Eqs. (B3) and (B4) with the rules given in Appendix A gives

$$\begin{aligned}\frac{V^{(a)}_{\text{eff},\delta^1}}{N}(\sigma_c, \eta_*, T, \mu) = \delta\frac{\lambda}{4\pi^2 N}\Bigg\{\eta_*^2\Bigg\{\frac{1}{4\epsilon^2} + \frac{1}{\epsilon}\Bigg[\ln\left(\frac{M}{\eta_*}\right) - I_2(\eta_*/T, \mu/T)\Bigg] + \Bigg[\ln\left(\frac{M}{\eta_*}\right) - I_2(\eta_*/T, \mu/T)\Bigg]^2 + \ln^2\frac{M}{\eta_*} \\ + \frac{\pi^2}{24}\Bigg\} + T^2 J_2^2(\eta_*/T, \mu/T)\Bigg\}.\end{aligned} \tag{B5}$$

Equations (B2) and (B5) give the total contributions from diagrams 1a, 1b, 1c, and 1d in Fig. 14.

To evaluate the contribution given by graph 2b in Fig. 14 we need to define the mass counterterm $D^{\delta}_{\text{exc}}\bar{\psi}\psi$ used to renormalize the exchange self-energy given by 3c. Note that the divergences are only associated with the terms proportional to the mass. This sets the Feynman rule to iD^{δ}_{exc}, where

$$D^{\delta}_{\text{exc}} = -\delta\frac{\lambda}{4\pi N}\eta\frac{1}{\epsilon}. \tag{B6}$$

Then, one can evaluate the one-loop contribution corresponding to 2b in Fig. 14,

$$\frac{V^{(a,c\ \text{term})}_{\text{eff},\delta^1}}{N}(\eta_*) = -i\int\frac{d^2p}{(2\pi)^2}\,\text{tr}\left[\frac{D^{\delta}_{\text{exc}}}{\not{p} - \eta_* + i\epsilon}\right], \tag{B7}$$

obtaining

$$\begin{aligned}\frac{V^{(a,c\ \text{term})}_{\text{eff},\delta^1}}{N}(\sigma_c, \eta_*, T, \mu) = \delta\frac{\lambda}{4\pi^2 N}\eta_*^2\Bigg\{-\frac{1}{2\epsilon^2} - \frac{1}{\epsilon} \\ \times\Bigg[\ln\left(\frac{M}{\eta_*}\right) - I_2(\eta_*/T, \mu/T)\Bigg] \\ - \ln^2\frac{M}{\eta_*} - \frac{\pi^2}{24}\Bigg\}\end{aligned} \tag{B8}$$

so that when adding the two contributions (B5) and (B8) the $1/\epsilon$ divergence as well as some finite terms cancel out, and only the $1/\epsilon^2$ divergence remains to be renormalized by zero point (vacuum energy) subtraction counterterms.

The Feynman renormalization coefficient corresponding to the linear counterterm $E^{\delta}\sigma$ is obtained from the divergent part of the fermionic loop contained in graph 3a of Fig. 14, namely

$$E^{\delta} = \delta\frac{\eta}{\pi\epsilon}. \tag{B9}$$

Then, adding all contributions one has

$$\begin{aligned}\frac{V_{\text{eff},\delta^1}}{N}(\sigma_c, \eta, T, \mu) = \delta\frac{\sigma_c^2}{2\lambda} - \frac{1}{2\pi}\Bigg\{\eta^2\Bigg[\frac{1}{2} + \ln\left(\frac{M}{\eta}\right)\Bigg] + 2T^2 I_1(\eta/T, \mu/T)\Bigg\} + \delta\frac{\eta(\eta - \sigma_c)}{\pi}\Bigg[\ln\left(\frac{M}{\eta}\right) - I_2(\eta/T, \mu/T)\Bigg] \\ + \delta\frac{\lambda}{N}\frac{\eta^2}{4\pi^2}\Bigg[\ln\left(\frac{M}{\eta}\right) - I_2(\eta/T, \mu/T)\Bigg]^2 - \frac{\eta^2}{2\pi\epsilon} + \frac{\delta}{\pi\epsilon}\Bigg[\eta^2 - \left(\frac{\eta^2}{4\epsilon}\right)\frac{\lambda}{4\pi N}\Bigg] \\ + X^{\delta}(\eta, \mu) + \frac{T^2}{4\pi^2}J_2^2(\eta/T, \mu/T).\end{aligned} \tag{B10}$$

The remaining divergent contributions come from purely vacuum (field independent) graphs and can be absorbed by the zero point energy subtraction counterterm

$$X^{\delta}(\eta, \mu) = \frac{\eta^2}{2\pi\epsilon} - \frac{\delta\eta^2}{\pi\epsilon}\left[1 - \frac{\lambda}{4\pi N}\left(\frac{1}{4\epsilon}\right)\right], \tag{B11}$$

finally giving the finite effective potential

$$\frac{V_{\mathrm{eff},\delta^1}}{N}(\sigma_c,\eta,T,\mu)=\delta\frac{\sigma_c^2}{2\lambda}-\frac{1}{2\pi}\left\{\eta^2\left[\frac{1}{2}+\ln\left(\frac{M}{\eta}\right)\right]+2T^2I_1(\eta/T,\mu/T)\right\}+\delta\frac{\eta(\eta-\sigma_c)}{\pi}\left[\ln\left(\frac{M}{\eta}\right)-I_2(\eta/T,\mu/T)\right]$$
$$+\delta\frac{\lambda}{4\pi^2N}\left\{\eta^2\left[\ln\left(\frac{M}{\eta}\right)-I_2(\eta/T,\mu/T)\right]^2+T^2J_2^2(\eta/T,\mu/T)\right\}, \tag{B12}$$

which is the result shown in Eq. (2.17). More details about renormalization within the LDE can be found in the first work of Ref. [6] (see also [24,25] for the GN model).

[1] D. J. Gross, R. D. Pisarski, and L. G. Yaffe, Rev. Mod. Phys. **53**, 43 (1981).
[2] M. Gleiser and R. O. Ramos, Phys. Lett. B **300**, 271 (1993).
[3] J. R. Espinosa, M. Quirós, and F. Zwirner, Phys. Lett. B **291**, 115 (1992).
[4] M. Moshe and J. Zinn-Justin, Phys. Rep. **385**, 69 (2003).
[5] A. Okopinska, Phys. Rev. D **35**, 1835 (1987); M. Moshe and A. Duncan, Phys. Lett. B **215**, 352 (1988).
[6] M. B. Pinto and R. O. Ramos, Phys. Rev. D **60**, 105005 (1999); **61**, 125016 (2000).
[7] H. F. Jones and P. Parkin, Nucl. Phys. **B594**, 518 (2001).
[8] V. I. Yukalov, Laser Phys. Lett. **1**, 435 (2004).
[9] J.-L. Kneur, A. Neveu, and M. B. Pinto, Phys. Rev. A **69**, 053624 (2004); J.-L. Kneur and M. B. Pinto, Phys. Rev. A **71**, 033613 (2005); B. Kastening, Phys. Rev. A **70**, 043621 (2004).
[10] J. O. Andersen, Rev. Mod. Phys. **76**, 599 (2004).
[11] E. Braaten and E. Radescu, Phys. Rev. Lett. **89**, 271602 (2002); Phys. Rev. A **66**, 063601 (2002).
[12] J.-L. Kneur, M. B. Pinto, and R. O. Ramos, Phys. Rev. Lett. **89**, 210403 (2002); Phys. Rev. A **68**, 043615 (2003).
[13] J.-P. Blaizot, R. Mendez-Galain, and N. Wschbor, Ann. Phys. (N.Y.) **307**, 209 (2003).
[14] O. Schnetz, M. Thies, and K. Urlichs, Ann. Phys. (N.Y.) **314**, 425 (2004); hep-th/0507120; Ann. Phys. (N.Y.) **321**, 2604 (2006).
[15] A. Barducci, R. Casalbuoni, M. Modugno, and G. Pettini, Phys. Rev. D **51**, 3042 (1995).
[16] L. D. Landau and E. M. Lifshtiz, *Statistical Physics* (Pergamon, New York, 1958), p. 482.
[17] N. D. Mermin and H. Wagner, Phys. Rev. Lett. **17**, 1133 (1966).
[18] S. Coleman, Commun. Math. Phys. **31**, 259 (1973).
[19] R. F. Dashen, S.-K. Ma, and R. Rajaraman, Phys. Rev. D **11**, 1499 (1975); S. H. Park, B. Rosenstein, and B. Warr, Phys. Rep. **205**, 59 (1991).
[20] M. Thies, J. Phys. A **39**, 012707 (2006).
[21] L. Jacobs, Phys. Rev. D **10**, 3956 (1974); B. J. Harrington and A. Yildz, Phys. Rev. D **11**, 779 (1975).
[22] U. Wolff, Phys. Lett. **157B**, 303 (1985).
[23] T. F. Treml, Phys. Rev. D **39**, 679 (1989).
[24] C. Arvanitis, F. Geniet, M. Iacomi, J.-L. Kneur, and A. Neveu, Int. J. Mod. Phys. A **12**, 3307 (1997).
[25] J.-L. Kneur and D. Reynaud, Phys. Rev. D **66**, 085020 (2002).
[26] S. K. Gandhi and M. B. Pinto, Phys. Rev. D **49**, 4258 (1994).
[27] S. K. Gandhi, H. F. Jones, and M. B. Pinto, Nucl. Phys. **B359**, 429 (1991).
[28] D. Gross and A. Neveu, Phys. Rev. D **10**, 3235 (1974).
[29] S. Coleman, *Aspects of Symmetry* (Cambridge University Press, Cambridge, England, 1985).
[30] R. Seznec and J. Zinn-Justin, J. Math. Phys. (N.Y.) **20**, 1398 (1979); J. C. Le Guillou and J. Zinn-Justin, Ann. Phys. (N.Y.) **147**, 57 (1983); V. I. Yukalov, Moscow University Physics Bulletin **31**, 10 (1976); W. E. Caswell, Ann. Phys. (N.Y.) **123**, 153 (1979); I. G. Halliday and P. Suranyi, Phys. Lett. **85B**, 421 (1979); J. Killinbeck, J. Phys. A **14**, 1005 (1981); R. P. Feynman and H. Kleinert, Phys. Rev. A **34**, 5080 (1986); H. F. Jones and M. Moshe, Phys. Lett. B **234**, 492 (1990); A. Neveu, Nucl. Phys. B, Proc. Suppl. **18**, 242 (1991); V. Yukalov, J. Math. Phys. (N.Y.) **32**, 1235 (1991); C. M. Bender *et al.*, Phys. Rev. D **45**, 1248 (1992); S. Gandhi and M. B. Pinto, Phys. Rev. D **46**, 2570 (1992); H. Yamada, Z. Phys. C **59**, 67 (1993); K. G. Klimenko, Z. Phys. C **60**, 677 (1993); A. N. Sissakian, I. L. Solovtsov, and O. P. Solovtsova, Phys. Lett. B **321**, 381 (1994); H. Kleinert, Phys. Rev. D **57**, 2264 (1998); Phys. Lett. B **434**, 74 (1998); for a review, see H. Kleinert and V. Schulte-Frohlinde, *Critical Properties of ϕ^4-Theories* (World Scientific, Singapore, 2001), Chap. 19; M. B. Pinto, R. O. Ramos, and P. J. Sena, Physica A (Amsterdam) **342**, 570 (2004).
[31] D. P. Menezes, M. B. Pinto, and G. Krein, Int. J. Mod. Phys. E **9**, 221 (2000).
[32] K. G. Klimenko, Z. Phys. C **50**, 477 (1991).
[33] J. I. Latorre and J. Soto, Phys. Rev. D **34**, 3111 (1986); A. Okopinska, *ibid.* **38**, 2507 (1988).
[34] P. M. Stevenson, Phys. Rev. D **23**, 2916 (1981); Nucl. Phys. **B203**, 472 (1982).
[35] R. Root, Phys. Rev. D **11**, 831 (1975).
[36] B. R. Zhou, Phys. Rev. D **57**, 3171 (1998); Commun. Theor. Phys. **32**, 425 (1999).
[37] R. M. Corless, G. H. Gonnet, D. E. G. Hare, D. J. Jeffrey, and D. E. Knuth, Adv. Comput. Math. **5**, 329 (1996).
[38] P. Forgacs, F. Niedermayer, and P. Weisz, Nucl. Phys. **B367**, 123 (1991).
[39] A. Chodos and H. Minakata, Nucl. Phys. **B490**, 687 (1997).
[40] J.-L. Kneur and D. Reynaud, J. High Energy Phys. 01 (2003) 14.
[41] J. I. Kapusta, *Finite-Temperature Field Theory* (Cambridge University Press, Cambridge, England, 1985); M. Le Bellac, *Thermal Field Theory* (Cambridge University Press, Cambridge, England, 1996).